Nimish Bhatt

Adhesion testing of cellulose fibres with polymer matrices

School of Engineering

Thesis submitted for examination for the degree of Master of Science in Technology.
Espoo 23.11.2016

Thesis supervisor:

Assistant Prof. Arttu Polojärvi

Thesis instructor:

Harri Santamala

Aalto University
School of Engineering

AALTO UNIVERSITY
SCHOOL OF ENGINEERING

ABSTRACT OF THE
MASTER'S THESIS

Author: Nimish Bhatt

Title: Adhesion testing of cellulose fibres with polymer matrices

Date: 23.11.2016 Language: English Number of pages: 5+67

Department of Applied Mechanics
Professorship: Aeronautical Engineering

Supervisor: Assistant Prof. Arttu Polojärvi
Instructor: Harri Santamala

In fibre reinforced composites, adhesion between the reinforcing fibres and matrix is fundamentally responsible for mechanical behaviour of a composite structure. The primary focus of this thesis is characterisation and measurement of Ioncell cellulose fibre adhesion with polymer matrix materials. The structure consists of two parts, theoretical review and experimental testing.

The theoretical section explains the concept of shear lag theory, which forms basis for stress transfer to fibres through matrix. A review of various micromechanical methods, mainly pullout, fragmentation and microdebond methods. Besides micromechanical methods, it also includes other methods using macro scale specimens. Experimental part consists of microbond tests. It includes specimen preparation, test set up, testing and finally results and analysis.

Keywords: Interface, Adhesion, IFSS, fibre-matrix, micromechanics, composites

Acknowledgements

This thesis concludes my studies in mechanical engineering at Aalto university. It posed diverse challenges and I am thankful to a lot of people who helped and guided me through it.

I would like to thank my supervisor, Professor Arttu for helping me through out, my instructor Harri, for giving me complete liberty to work on the topic on my own. I am also grateful to professor Olli for having faith in me with the topic. I would also like to thank everyone in the lightweight structures lab for their guidance and help without which, this would not have been possible. I would also like to thank professor Jyrki at Tampere university of technology, to let me use the facilities in the materials lab.

Finally, I am also grateful to my family and friends for their support.

Otaniemi, 23.11.2016

Nimish Bhatt

Contents

List of Tables

List of Figures

List of symbols

α	Coeffcient of thermal expansion
β	Constant called Nayfeh's parameter
γ	Surface energy
ν	Poisson's ratio
π	Constant pi
σ	Stress: Tensile or compressive
τ	Shear stress
θ	Contact angle of liquid droplet on a flat surface
d	Diamter of fibre
E	Young's modulus of elasticity
F	Force
G	Shear modulus of rigidity
L_e	Embedded length of fibre in matrix
L_{ce}	Critical embedded length
s	Ratio of fibre length to diameter
T	Temperature
V	Volume fraction
W_a	Thermodynamic work of adhesion

1 Introduction

Many materials existing in nature are composite materials consisting of two or more constituents like wood, which consists of approximately 50% cellulose in fibrous form, (23 to 33)% lignin as a matrix, hemi-celluloses and small amounts of external content [21]. Composite materials are more efficient in terms of strength to weight ratio, tailorability to requirement. Carbon and glass fibre reinforced composites (FRC) are used for high performance applications but are difficult to separate into constituents at the end of life for recycling. Thus, resulting into land fills causing adverse environmental impact [22].

At present natural fibres are widely used for automotive interior panels by several automotive companies. Figure 1a shows Mercedes Benz S class interiors made using hemp fibres. The advantages of natural fibres are 60% less energy for production compared to glass fibres, cause less wear to the processing equipment, lower health risks and are easy to work with. Natural fibres could improve fuel efficiency in automotive by 25% weight reduction, thereby saving 250 million barrels of crude oil per year

(a) **(b)**

Figure 1: (a) Interior panels of Mercedes Benz S class made from hemp fibres and (b) Wind turbine blades made from flax fibres

[23, 24]. More demanding applications like the wind turbine shown in the Figure 1b are emerging.

In past few decades, there has been a growing interest in research focused on natural fibres, and using it as a reinforcement in biodegradable polymer matrix materials like PLA to develop biodegradable composite materials. Also more commonly known as biocomposites. Natural fibres have advantages over conventional reinforcing materials like low cost, low density, acceptable specific strength and biodegradability. However, natural fibres are hydrophilic whereas, polymer materials are hydrophobic and hence are not compatible with each other readily [25].

Natural fibres available from various plant sources have more defects compared to synthetic fibres and their strength properties vary depending on where they are grown [22, 26]. Whereas, man made natural fibres produced from regenerated cellulose are consistent in properties and physical characteristics. Moreover, the performance of composite materials is largely governed by fibre architecture and geometry, which makes man made natural fibres a preferred choice.

1.1 Objectives and scope

The objective of this thesis is to measure interfacial adhesion of Ioncell cellulose fibres with commercial polymer matrices. Many micro-mechanical methods have been developed [27] but none of the methods has been adopted by engineering standards. Most of these methods require specialised equipment for micro-mechanical tests. Hence, a secondary objective was to develop or evalute one of the existing methods which could be performed using standard equipment in lightweight structures laboratory.

During initial literature research, it was discovered that results obtained from these methods suffer from data scatter. The methods are also sensitive to materials being tested and test parameter, even across different studies using the same method [28]. Hence it became paramount to ensure that, the method selected was suitable taking into account Ioncell fibre and polymer matrix properties. Also, to analyse probable

causes of data scatter for the selected test to ensure reliable results.

1.2 Structure

This thesis is composed of two parts, review and experiment. The review consists of fundamental theory governing fibre/matrix adhesion, various methods based on it with improvement over the years. Comparison of methods so as to select a suitable one as per the scope and objective. Finally, experimental part of actual testing for measurements and evaluating the validity of testing method.

2 Fibre/matrix adhesion: Theory and test methods

The concept of load transfer and load sharing between the constituents of composite materials is fundamental to understanding the behaviour of composites. The load shared by fibre and matrix can be calculated based on the volume fraction of each constituent in the given specimen. The reinforcement can be considered as acting effectively, if the majority of the load acting on the composite is borne by the reinforcement. This results into higher strength and stiffness of the material, since the reinforcement is stiffer and stronger than the matrix [2].

The analytical methods used for composite analysis can be used to predict the composite properties in fibre direction by applying the simple rule of mixtures. However, this model has limited practical use since in structural applications there are often loads acting at an angle in addition to the loads in fibre direction. In such a case, fibre matrix adhesion plays an important role in load bearing capacity of structural element [29].

The mechanical properties like transverse tensile strength for unidirectional composites and delamination resistance, are largely influenced by fibre/matrix adhesion [3]. Apart from that, properties like shear strength, compressive strength and fatigue resistance are also affected by fibre/matrix adhesion at micro level [3]. Thus, fibre matrix bond at microlevel would enable better understanding of composite mechanical behaviour.

2.1 Fibre/matrix interface

The fibre matrix bond strength at the interface is affected by several bonding mechanisms which are described in subsection 2.1.1. At present, there is no widely accepted method for characterizing fibre/matrix interface and several methods have been used for it so far. These methods can be classified into single fibre and multi fibre methods. Multi fibre methods would include specimens that use mutiple fibre in mat or bundle

form. Both the approaches have their own advantages and disadvantages, single fibre methods are easier to perform and enable direct measurement of interfacial properties but they don't represent an actual composite, whereas, multi fibre methods represent actual composites but the tests are more tedious and the interfacial properties measured are indirect [30]. Moreover, the results are dependent on specimen geometry, fibre/matrix volume ratio [31]. However, even though single fibre methods do not represent a composite material, they can be used for relative comparison of various fibre matrix combinations and to study various fibre treatments to improve adhesion [30, 5].

2.1.1 Fibre matrix bonding mechanisms

It is essential to understand different bonding mechanisms occurring in fibre reinforced composite, before studying different methods for measuring the bond strength. This section describes various bonding mechanisms which influence the bond strength of composites [2].

Absorption and wetting: Wetting occurs when solid comes in contact with a liquid giving rise to a solid liquid interface formation as shown in Figure 2. Absorption is accompanied by wetting. The ease with which this interface forms is dependent of Van Der Waals forces. The thermodynamic force responsible for this wetting is expressed as. work of adhesion. It can be calculated by Dupre's equation as follows,

$$W_a = \gamma_{SV} + \gamma_{LV} - \gamma_{SL} \tag{1}$$

In equation (1), γ are the surface energies, whereas subscripts S,L and V represent solid, liquid and vapour respectively. The contact and formed by a droplet in contact with a solid is given by Young equation,

$$\gamma_{SV} = \gamma_{SL} + \gamma_{LV}\cos\theta \tag{2}$$

These surface energies are known for solids and liquids which in this case is fibres and matrices. Wetting occurs better when the surface energy for fibre is higher than the surface energy for matrix. This is important for manufacturing of composites since better wetting promotes adhesion by easier impregnation of fibres with the matrix.

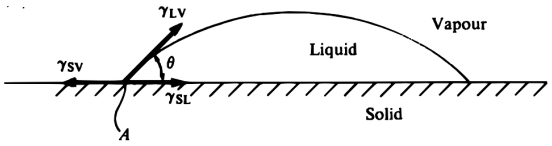

Figure 2: Liquid drop in contact with a solid surface. Contact angle θ, and surface energies λ [2]

Interdiffusion and chemical reaction: The adhesion can be improved by diffusion at the interface. Diffusion of free molecular chains can be seen in Figure 3. This effect is can be employed by treating fibre surface with a coupling agent. Also various types of chemical reaction involving formation of covalent or ionic bonds can be used to improve adhesion as shown in Figure 4. These bonding mechanisms can be utilized by sizing applied on the fibre during the manufacturing process.

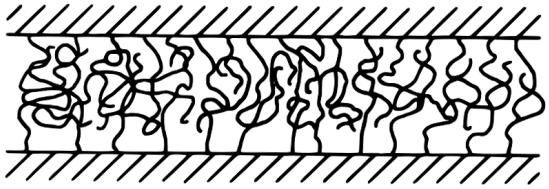

Figure 3: Interdiffusion and molecular entanglement [2]

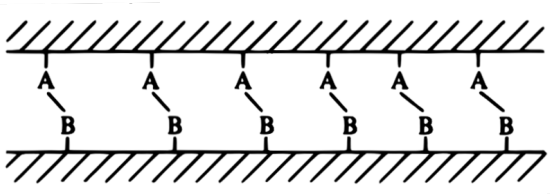

Figure 4: Chemical reaction [2]

Electrostatic attraction: Surfaces charged with opposite polarity attract each other. If he surfaces are charged with opposite polarity as shown in Figure 5, adhesive force can exist. Again surface treatments on fibres can be used to improve this further. Also various chemical treatments can be used to improve electrostatic attraction, it is unlikely that this can significantly increase the bond strength.

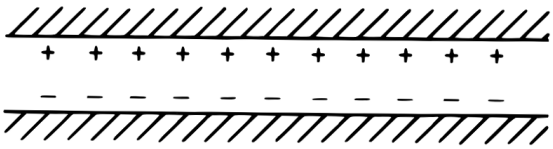

Figure 5: Electrostatic attraction [2]

Mechanical keying: Mechanical keying occurs due to microscopic surface irregularities on the fibre surface as shown in Figure 6. This can be further improved by good wetting. The increase in contact area can further improve the adhesion. Thus, improving performance of composite in longitudinal direction. This effect can result in higher shear stress at the fibre/matrix interface.

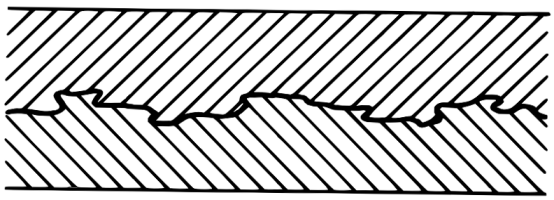

Figure 6: Mechanical keying [2]

Residual stresses: Residual stresses arise from volume changes due to the phase transformation of matrix as well as due to thermal contraction for resins cured at elevated temperatures. Main source of residual stresses is cooling during the manufacturing of composites. The coefficient of thermal expansion for matrix materials is usually higher than the fibres. This results in compressive stresses on fibres and tensile stresses on matrix.

2.1.2 Interface and interphase

Interface is the two dimensional surface that forms around the fibre, where fibre comes in contact with the matrix material. Most methods developed for measuring adhesion at microlevel measure interfacial strength of this interface. However, there are studies that report a three dimensional space around the fibre which has properties different from both the fibre and the matrix [32], and is known as interphase. This phase change occurs due to the chemical interaction between fibre/matrix that occurs due to the surface treatments applied on the fibre.

2.1.3 Shear lag model

The stiffness of fibres is higher than matrix material in fibre reinforced composites and fibres carry most of the load in the longitudinal direction. When a composite is axially loaded, due to the lower stiffness of the matrix, the load is transferred to fibres through matrix by means of shear [3] at the interface. The theory to explain this interaction of forces was first proposed by Cox in 1952 is commonly known as the shear lag theory which still forms basis for many recent models.

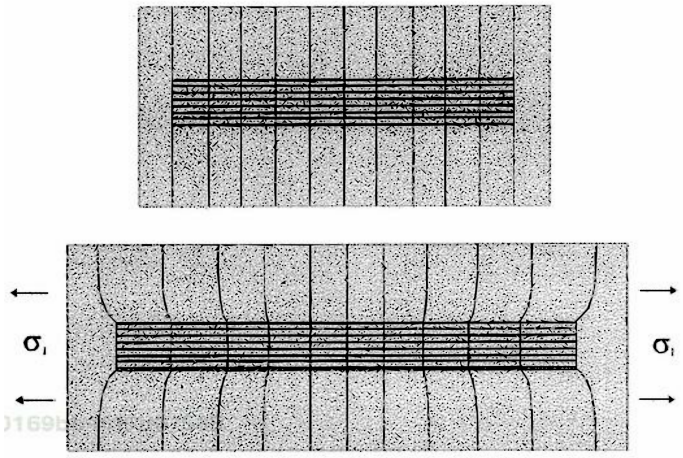

Figure 7: Composite with (top) and without stress (σ_1) (bottom) [3].

For a composite loaded in tension as shown in Figure 7, the distribution of shear stress at the interface and tensile stress in fibre can be seen in Figure 8. These stresses

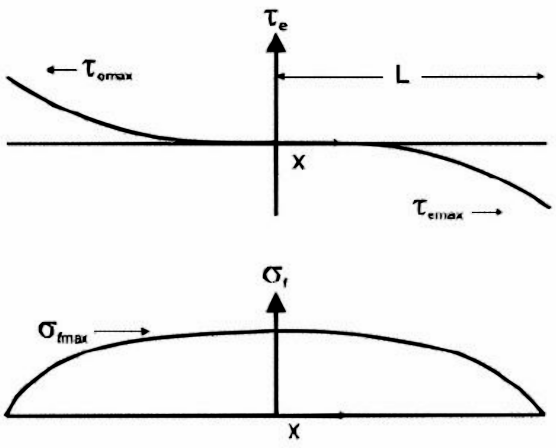

Figure 8: Distribution of interfacial shear stress (τ) (top) and tensile stress (σ)in the fibre (bottom) respectively. L is half of total length [3].

are given by Equations 3 and 4.

$$\sigma_f = E_f \epsilon_1 \left\{ 1 - \cosh\left(\frac{nx}{r}\right) / \cosh(ns) \right\} \tag{3}$$

$$\tau_e = \frac{1}{2} n E_f \epsilon_1 \sinh\left(\frac{nx}{r}\right) \cosh(ns) \tag{4}$$

$$n^2 = \frac{2E_m}{\left\{ E_f (1 + \nu_m) \ln\left(\frac{P_f}{V_f}\right) \right\}} \tag{5}$$

Here, x is the distance from end, s is fibre aspect ration, r is fibre radius and n is a dimensionless parameter given by Equation 5. Fibre aspect ratio, s is ratio of fibre length to diameter. σ_f and τ_e are tensile and shear stressen in fibre and matrix respectively. ν is Poisson's ratio and v is volume fraction in composite. Suffixes f and m represent fibre and matrix respectively. The Equations 3 and 4 can be used to predict the stress transfer over the length of the embedded fibre. These equations are derived based on the assumption that the bond is perfect so that the stress transfer occurs through the interface without any slip or yielding, and materials are loaded within the elastic limit.

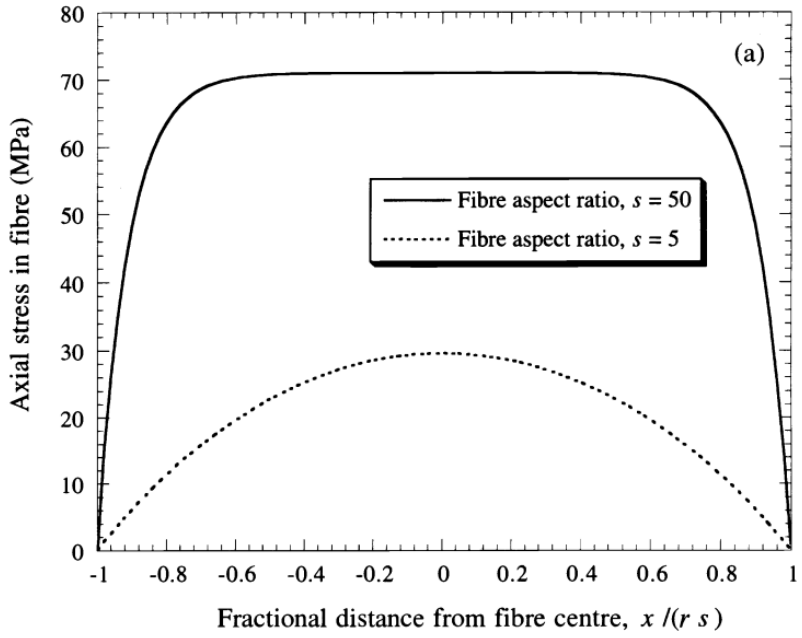

(a) Tensile stress

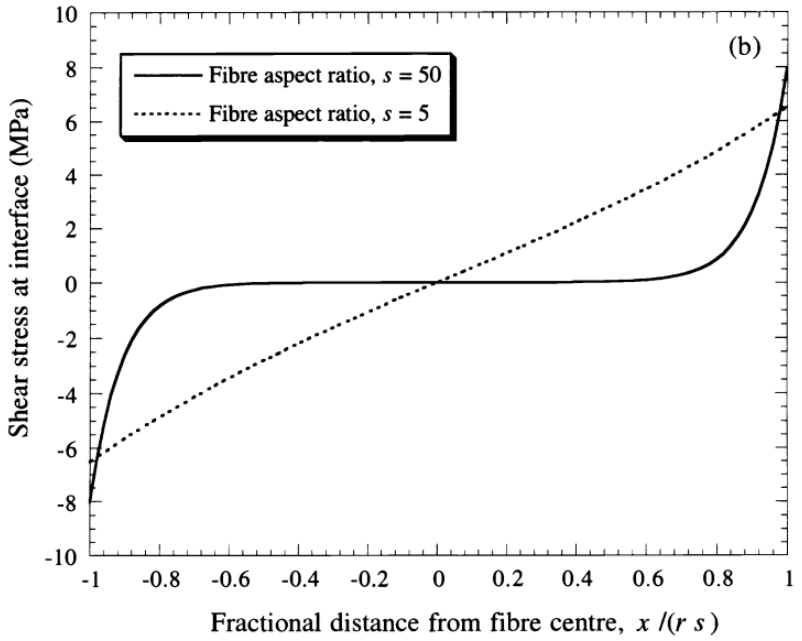

(b) Shear stress

Figure 9: Predicted stress distribution along the length [4].

Figure 9a and 9b show the predicted variation of tensile and interfacial shear stress respectively for a glass fibre in polyester composite for two different aspect ratios [4]. It is apparent from the figures that the peak tensile stress occuring at the centre of

fibre is a function of length, and for long fibre, there is a plateau region where tensile stress in maximum where as interfacial shear stress is zero. This leads to concept of stress transfer length. The fibre with the aspect ratio of s=5 is not long enough to build a plateau region. Hence fibres with low aspect ratios do not provide efficient reinforcement because they carry much less load compared to longer fibres in the same composite.

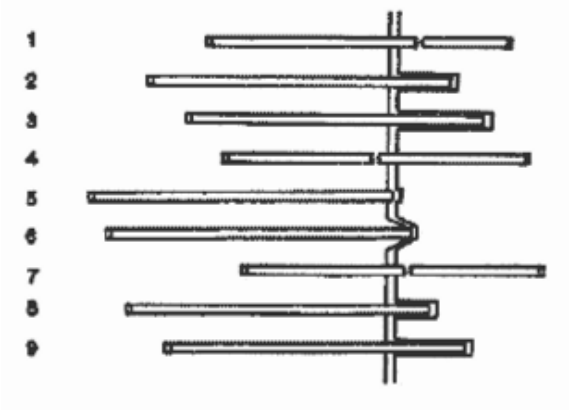

Figure 10: Crack propagating in a unidirectional composite [3]

Before going into methods for measuring fibre/matrix adhesion, it is important to understand the concept of critical fibre length. In Figure 10, the crack is perpendicular to the fibre direction and the horizontal fibres are numbered. The fibres, 2,3,8 and 9 are debonded where as the fibres 1,4 and 7 have failed. Assuming that pull out is resisted by shear stress at interface [3]. Now, considering a constant value of shear stress τ_i averaged for the variation over embedded length L_e,

$$\sigma_f = \frac{2\tau_a L_e}{r} \tag{6}$$

From equation 6, increase in the value of embedded length (L_e) will increase the stress (σ_f) induced in the fibre and if this stress value exceeds the tensile stress of the fibre, it will cause the fibre to fail. However, if the embedded length is too small, and the induced tensile strength is less than tensile strength of the fibre, the debonding occurs and fibre is pulled out. The length at which the induced stress is equal to the

maximum tensile strength of the fibre, is called critical length of the fibre. For fibre with ultimate tensile strength of σ_{fu}, Equation 6 will become,

$$\sigma_{fu} = \frac{2\tau_a L_{ce}}{r} \tag{7}$$

The critical length of the fibre will be $2L_{ce}$ as shown in Figure 11. Thus, critical length for a given fibre matrix system can be calculated if the interfacial stress,fibre tensile strength and fibre diameter are known.

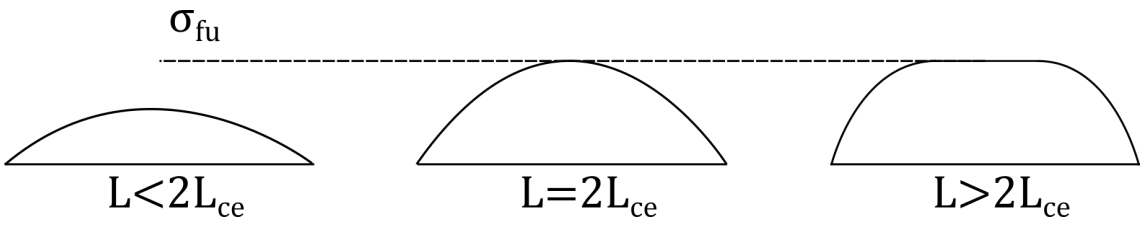

Figure 11: Embedded lengths (l), critical embedded length (l_{ce}) and tensile stress (σ) distribution in fibre

2.2 Single fibre test methods

Most methods used for measuring adhesion involve measurement of shear strength at fibre/matrix interface in case of single fibre tests while complete laminates can be tested by using methods that induce interlaminar shear stresses [2]. Single fibre tests measuring interfacial shear stress are also infuenced by friction and can lead to exaggerated values of measured shear stress. The methods discussed in this section include pull-out, fragmentation and indentation method. These methods have been widely used for various types of composite materials like fibre reinforced composites (FRC), ceramic matrix composites (CMC) and metal matrix composites (MMC). Also variations of these methods and development over the years with their advantages and disadvantages.

2.2.1 Pull-out tests

The pull out method is one of the oldest methods for testing fibre/matrix interface [6]. In the pull out method, short lengths of fibre are embedded in matrix and allowed to cure. Once the specimen is cured, the embedded length is determined using a microscope. Then, the fibre is pulled out from the matrix while recording the force and displacement of the fibre. In this method, it is important to to keep the embedded length of the fibre short enough to ensure shear failure at interface. If the embedded length is greater than critical embedded length, the fibre fails in tension before the interfacial failure. Different variations of matrix geometry include cylindrical blocks and hemispherical droplets on a flat surface as shown in figure 12 [27]. Variations of single fibre pull out method have been developed overtime. Some of these methods are described below.

Microbond method is one of the variations of the pull out method [31]. In this method, the matrix is in form of a micro droplet on a fibre as shown in the Figure 12b. This method is advantageous in specimen preparation compared to the conventional pull out method. The embedded length of the fibres is often in the range of 50 to 250 microns for pull out methods [33], which can be challenging to achieve in a matrix mould due to meniscus effects. On the other hand, controlling diameter of a droplet to such dimensions is relatively easy, and the effects of meniscus are reduced in a micro droplet since the surface of the droplet minimizes due to surface tension effects [31]. Moreover axis-symmetric droplets can be obtained by this method, reducing geometrical variation between specimens [34]. The rest of the test procedure is similar to the pull out method.

Although microbond technique is relatively easy compared to other methods, one of the major challenge is achieving droplet size required for interfacial failure to get successful test results. Also achieving accurate droplet size over a range of specimens is challenging due to the microscopic scale. The droplet size also influences the droplet symmetry [34], which influences test results. The blade gap is responsible for the stress

state in the droplet and variation in blade gap results into a change in this stress state in the droplet. The peak force measured increases with the increase in blade gap [35].

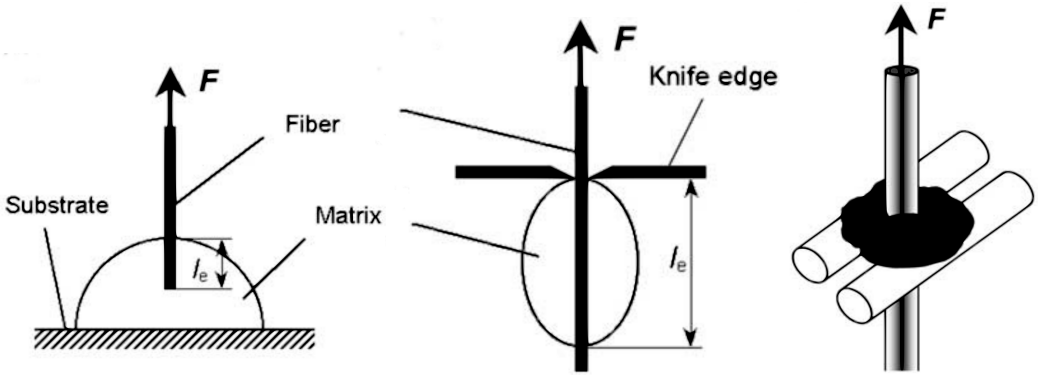

(a) Pull out test **(b)** Microbond test **(c)** Three fibre test

Figure 12: Schematic of various pullout methods. L_e is the embedded length of fibre [5]

The three fibre method is another variation of the conventional pull out method, as shown in the Figure 12c. In this method, two horizontal fibres are covered with the resin selected for the study. The fibre selected for study is then passed in between the horizontal fibres and then the two horizontal fibres are brought close to each other so that a small part of the vertical fibre in proximity of horizontal fibres, is immersed with resin [36]. Jarvela et. al. also attempted this method but, with a different specimen preparation technique [37]. They directly applied a small droplet of resin selected for the study, to the vertical fibre instead of the two horizontal fibres. The two horizontal fibres, were then made to come in contact with the resin drop, while taking care that none of the fibres came in contact with each other. The remaining testing procedure is similar to the pull out test.

$$\tau_a = \frac{F_{max}}{\pi d l_e} \tag{8}$$

The data obtained from tests is in form of force-displacement curve. The shear strength of the bond is calculated using stress based approach using equation 8. F_{max}

is the maximum force recorded, d is the fibre diameter and l_e is the embedded length. This shear stress is often referred to as apparent interfacial shear stress, since it is averaged over the whole embedded length. This apparent interfacial shear strength (τ_a) is influenced by friction and thermal shrinkage which can lead to higher values of force measured resulting in higher shear strength.

Over the years there have been improvements on the shear lag theory developed by Cox to include effects of friction and thermal shrinkage, typically observed in fibre reinforced composites using polymer resins. Also, many studies indicate that in pull out tests, interfacial failure occurs by crack propagation at the interface [1].

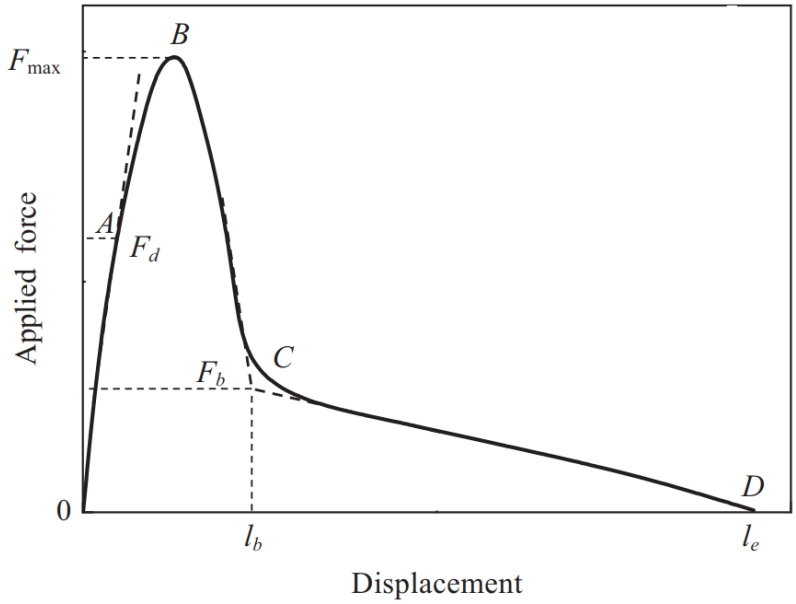

Figure 13: Idealized force displacement curve with [1]

Figure 13 highlights features, indicating various stages of interfacial debonding. Debonding starts when the force exceeds a certain value called debond force (F_d). Following this, the crack progresses along the embedded length through the interface with increase in force. The friction between the matrix and fibre contributes to the adhesional force measured. This measured force increases to a maximum value of F_{max} which can be much higher than the debond force (F_d). Once the embedded length of the fibre is reduced to a certain point the force starts decreasing and finally drops to

a value F_b, at which all embedded length is debonded. The remaining portion of the curve is force due to friction between the fibre and the matrix.

There are two theoretical approaches used for characterizing fibre/matrix interface in pull out tests. Energy based approach and stress based approach. In energy based approach, the critical energy release rate is used whereas, in stress based approach local interfacial shear stress (IFSS) is used for characterizing interface. The two approaches have been discussed and verified experimentally, both have been found suitable to characterize interfacial adhesion [1, 38]. Debond force (F_d) is the key parameter for both approaches [39]. The most recent model to calculate debond stress based on debond force (F_d) is as follows,

$$\tau_d = \frac{F_d \beta}{2\pi r_f} \cosh(\beta l_e) + \tau_t \tanh \frac{\beta l_e}{2} \tag{9}$$

where,

$$\tau_t = \frac{\beta r_f E_f}{2} (\alpha_f - \alpha_m) \Delta T \tag{10}$$

$$\beta^2 = \frac{2}{r_f^2 E_f E_m} \left\{ \frac{E_f V_f + E_m V_m}{\frac{V_m}{4G_f} + \frac{1}{2G_m}(\frac{1}{V_m} \ln \frac{1}{V_f} - 1 - \frac{V_f}{2})} \right\} \tag{11}$$

Equation 10 for τ_t is the stress due to thermal shrinkage and equation 11 for β is shear lag constant called Nayfeh parameter which is replacement over the original Cox parameter because it gives correct results for microbond specimens [40]. In Equations 10 and 11, α is coefficient of thermal expansion, E is elasticity modulus, V is volume fraction and G is longitudinal shear modulus. Shear modulus of rigidity requires some additional apparatus for measurement. Suffixes 'f' and 'm' are for fibre and matrix materials respectively. The above model requires the value of debond force from the test which can be measured if the complete system consisting of the specimen, materials and the test equipment, are stiff enough so that small kink due to debonding can be identified as change in slope in the force-displacement plot, as shown in figure 14.

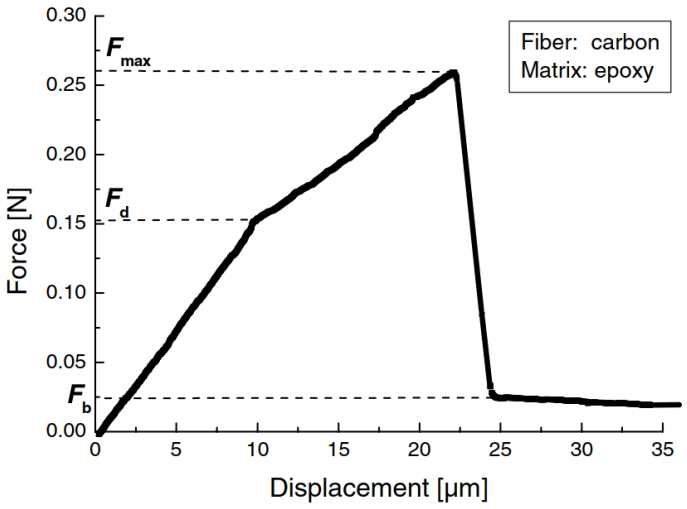

Figure 14: A force-displacement curve recorded during pull-out test [5]

However, the kink that is visible in the figure 14 plot, is not clearly distinguishable or even impossible to discern, depending on elasticity of materials used. This may occur in natural fibres since elasticity of natural fibres is much less compared to carbon fibres. In such cases, indirect estimation of debond force can be done using a model developed by Zhandarov et. al. [40, 1]. This model is based on shear lag theory and takes into account the effects of thermal shrinkage and friction on interfacial shear stress. Equation 12 based on this model can be used for indirect estimation of debond force from maximum force (F_{max}).

$$F_{max}(l_e) = \begin{cases} \frac{2\pi\tau_f}{\beta}\left[\tau_d \tan(\beta l_e) - \tau_t \tan(\beta l_e)\tanh\left(\frac{\beta l_e}{2}\right)\right] \\ \text{for} \quad \beta l_e < \ln(u + \sqrt{u^2 - 1}) \\ \frac{2\pi\tau_f}{\beta}\tau_d \frac{u}{\sqrt{u^2+1}} - \tau_t\left(1 - \frac{1}{u^2+1}\right) + \tau_f[\beta l_e \ln(u + \sqrt{u^2+1})] \\ \text{for} \quad \beta l_e \geq \ln(u + \sqrt{u^2+1}) \end{cases} \tag{12}$$

where,

$$u = \frac{\sqrt{\tau_t^2 + 4\tau_f(\tau_d - \tau_f)} - \tau_t}{2\tau_f} \tag{13}$$

$$\tau_f = \frac{F_b}{2\pi r_f (l_e - l_b)} \tag{14}$$

The interfacial friction (τ_f), can be found from F_b on CD part of the force displacement curve, as shown in the figure 13. In most of the pull-out tests, the tail part (CD) of the force displacement curve is discernable, thus frictional stress (F_b) can be determined. In case the debond force (F_d) is not discernable, equation 12 can be used to estimate debond stress (τ_d). Table 1 shows results comparing directly and indirectly measured debond stresses (τ_d) for different fibre/matrix combinations. The first case is when debond force (F_b) is discernible on force displacement plot from the experiment. The second case is indirect estimation of debond stress using the Equation 12. In cases where frictional force (F_b) is not discernable on the force displacement plot, it can be estimated using method presented in [5]. The values of τ_d calculated indirectly are close to τ_d calculated directly using F_d but some error is observed. This indirect estimation is recommended only when the debond force F_d cannot be reliably measured.

Table 1: Local interfacial shear stress and frictional stress calculated using three different approaches using Equations 9 and 10 (in MPa) [1].

			Fibre/matrix systems	
Approaches		**Units**	**E-glass/PP**	**Carbon/PA 6.6**
1	From F_d and F_{max}	MPa	τ_d=18.3±3.4	τ_d=37.3±19.2
		MPa	τ_f=2.4±1.3	τ_f=17.7±23.2
2	From F_b and F_{max}	MPa	τ_d=16.2±3.7	τ_d=48.8±30.1
		MPa	τ_f=3.3±1.4	τ_f=5.6±2.0
Difference		%	τ_D: 11.5±0.09	τ_D: 30.83±56.7
			τ_f: 27.3±0.08	τ_f: 68.36±91.4

2.2.2 Fragmentation method

This method, also known as single fibre composite test, was first used by Kelly and Tyson [41] to study how properties of a composite depends on the individual properties of reinforcement and matrix material. They used copper as the matrix material with tungsten and molybdenum as reinforcement. On applying strain to the composite, they observed the fibres fracturing at multiple points where the maximum fibre tensile strength (σ_{fu}) is reached, and upon increasing the strain, the number of broken fibre fragments kept increasing to a point where fragment lengths are too small for shear stress transfer to build up enough tensile stress. This final length of the fibre is called critical length. The concept of critical length here is same as discussed before. It is the length required for stress transfer so that the tensile stress in fibre equal to ultimate fibre tensile stress (σ_{fu}). Thus, the shorter the critical length, better is the adhesion between the fibres and matrix. Figure 15, shows stages in progression of fragmentation test with increase in load and decrease in fragment lengths to critical length (L_c).

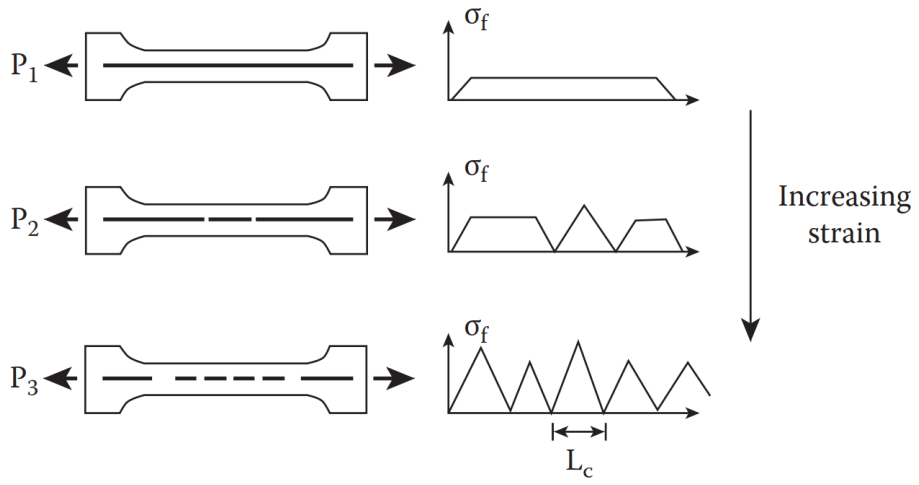

Figure 15: Axial stress distribution in fibres during fragmentation process based on Kelly Tyson's model [6]

The loading of specimen used in fragmentation test is shown in the figure 16. The dog-bone shaped specimen shown in the Figure 16, is commonly used for this test. The dog bone shaped specimen in manufactured using a mould. For manufacturing the

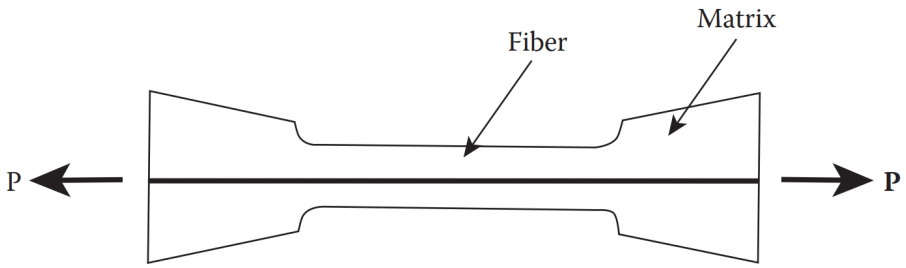

Figure 16: Single fibre fragmentation test schematic [6].

specimen, a single filament of fibre is suspended between two points in the mould cavity with certain amount of pre-tension. Pre-tension is done to compensate for thermal shrinkage during the curing process and to keep the fibre straight. Liquid resin is then poured in the mould cavity until it is full. After that curing follows as per the resin used. Once cured the specimen is polished so that it is transparent and the fibre inside is visible.

For testing, the specimen is loaded in tension and strain is applied in multiple stages. After each stage the specimen is held at that strain level for a certain amount of time till the fragmentation stabilizes at that strain. Ultimately the test is stopped when applying more strain does not result in further fragmentation. During test, a microscope is used to monitor the fragmentation process and upon saturation the fragment lengths are measured. [42, 7]. Matrix material, when loaded exhibits birefringence, this property is used to observe photoelastic stress distribution under polarized light. It also makes fibre breaks easier to observe during the test. Figure 17, shows photoelastic stress distribution around carbon and glass fibre specimens in epoxy resin [7]. Apart from visual inspection, acoustic emission technique has also been developed for monitoring fragmentation process and measuring fragment lengths [27].

It is important that strain to failure for matrix material is higher than strain to failure for the reinforcing fibres for this test to be successful and usually it is the case for most fibre reinforced composites. This makes it a good choice. Strain to failure ratio of fibre to matrix of three or higher is usually preferred to avoid matrix failing prematurely during the test [3]. The shear stress at the interface is assumed to be

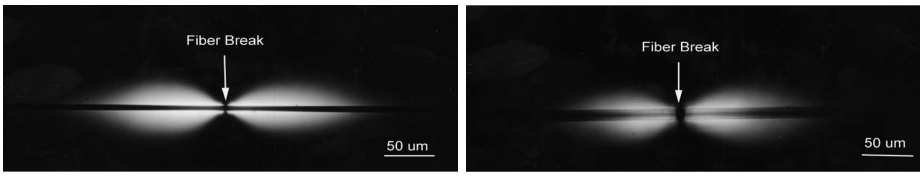

(a) Carbon fibre **(b)** Glass fibre

Figure 17: Photoelastic birefringence showing stress distribution at fibre breaking point [7]

constant along the length and the critical length. From this length and the tensile stress of the fibre, interfacial shear stress can be derived by simple force balance.

$$(\tau_a) = \frac{\sigma_f d_f}{2\bar{l_c}} \tag{15}$$

σ_f is fibre tensile stress, d_f is the diameter of fibre and $\bar{l_c}$ is the critical length in Equation 15. Note that the critical length here will the the average of lengths of fragments obtained at the end of fragmentation test.

While this method was originally developed using metal matrix composites, it was first used by Drzal et. al. in 1980 for fibre reinforced composites [6]. Although theoretically this method sounds simple, there are many factors that influence the test results. The interfacial strength measured is related to maximum fibre tensile strength. All fibres have variation in strength due to defects resulting from manufacturing or handling or internal anomalies. These randomly located defects result in variation in strength in fibres which cause uncertainties in fibre failure depending on the average stress during the test. During the test, any fragment longer than critical length will split further into two fragments while fragments smaller than critical length will stay as they are. In the end, all the fragment lengths will lie between l_c and $l_c/2$. This variation in lengths of fragments is random and often Weibull distribution is used to determine average value of critical length [27, 43]. An alternate simplified approach is to assume a uniform distribution of fragments and calculate the average critical length as shown

in equation 16 [42, 44].

$$\bar{l_c} = \frac{4}{3} l_c \tag{16}$$

Figure 18 shows a typical data plot from a fragmentation test. The crack density is

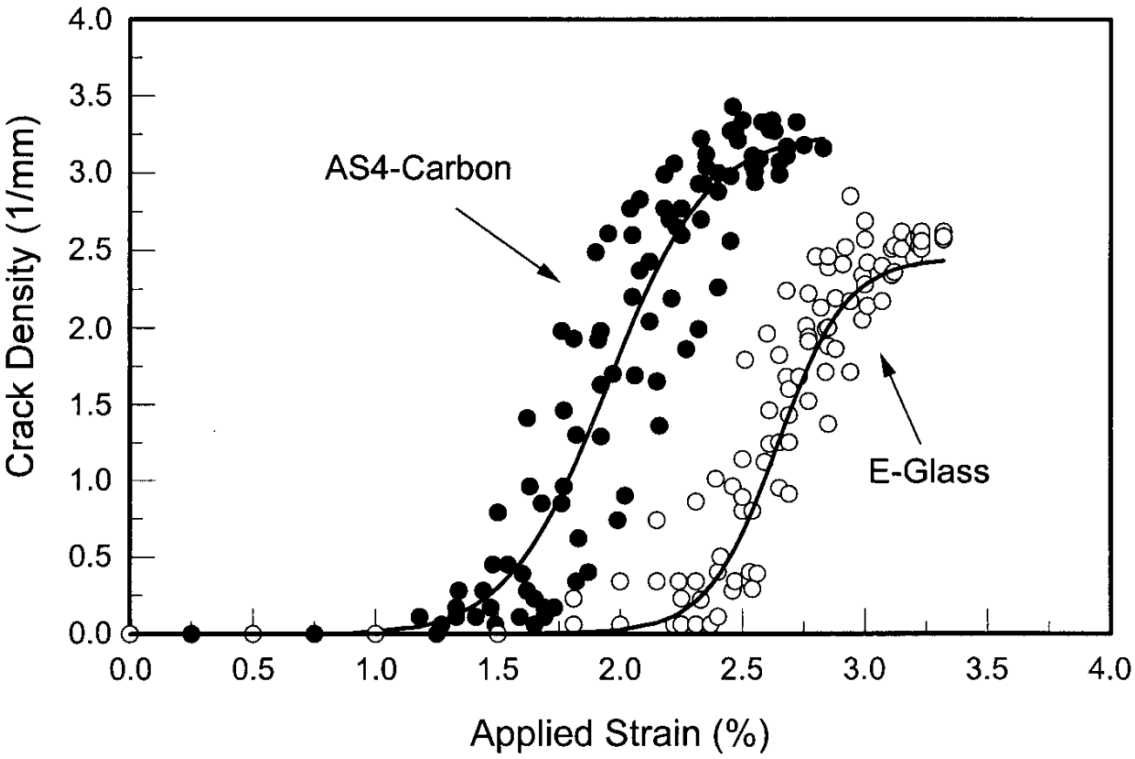

Figure 18: A data plot of crack density against applied strain from a fragmentation test [7]

number of cracks per mm, carbon fibre specimen was given five min after applying strain where as glass fibre specimen was given twenty min [7].

The primary advantage of this method is that the specimen and loading is similar to an actual composite unlike the pull-out method, as in that the load is applied to matrix. A fragmentation test provides in-situ information on both, statistical fibre strengths at small gauge lengths and fibre/matrix interfacial properties at the same time. The interfacial strength is a function of fibre tensile strength according to equation 15. Testing fibres at very small gauge lengths is difficult and often the strength is extrapolated from longer gauge lengths based on statistical models [27].

2.2.3 In-situ methods

As the name suggests, these methods measure interfacial strength in-situ, meaning in original place. The tests discussed so far, require specimens that are specifically prepared for the test, and differ from a real composite. In-situ tests use specimens obtained from actual composite manufactured using conventional techniques.

Microdebonding was originally developed by Mandell et. al. [8], allows in-situ measurement of interfacial adhesion. This test is similar to indentation test used for measuring hardness of metals. The authors tested glass, aramid and graphite fibres in epoxy matrices for interfacial strength measurement. The specimen is prepared from a regular composite by polishing it with fibres normal to the surface. A steel probe is gradually used to apply certain load on the surface followed by microscopic inspection for interfacial failures. The load is then increased till the failure is observed across single or multiple fibres. The test is then repeated on different areas to get statistically significant sample size [8]. This test has been widely used for metal matrix composites and ceramic matrix composites [45].

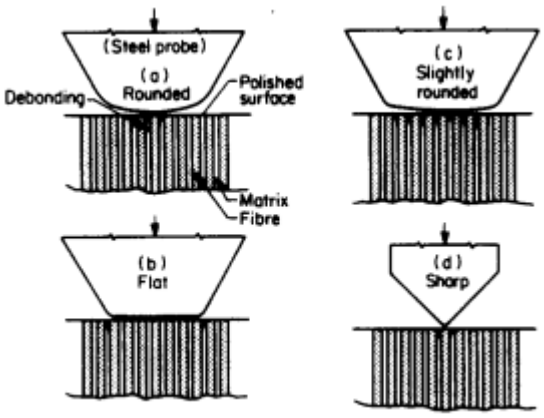

Figure 19: Probe geometries used by Mandell et. al. [8]

Different probe geometries used are shown in figure 19. The tests were conducted on a modified Vickers microhardness tester. With the rounded and slightly rounded tips debonding a single fibre also results in distribution of the load over a larger surface

making analysis difficult. The flat tip requires accurate alignment for good results. The sharp tip provided good results for single fibre debonding but the loads were less than one gram. The sharp tip provided the best results in testing and data analysis. It was easier to align due to its smaller size. Data analysis also was simpler since all the load is transferred to the fibre.

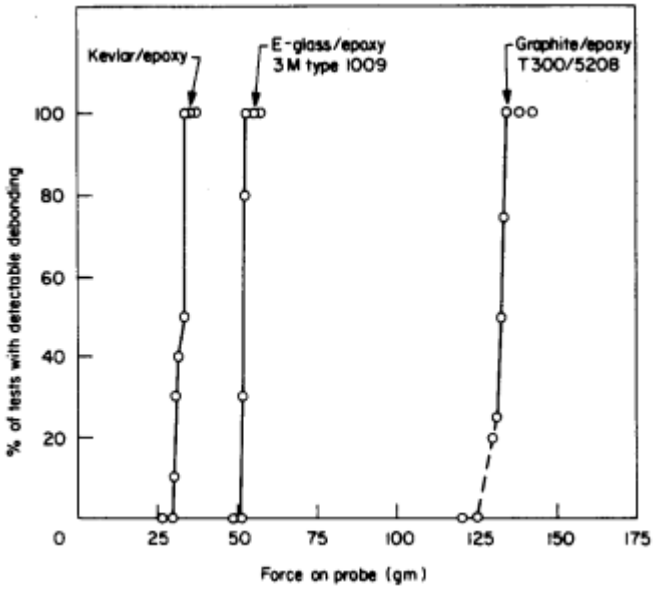

Figure 20: Results from microdebonding test [8]

The results of study by Mandell and et. al. are shown in figure 20. They found out that the results were reproducible as long as same probe was used however there was some variation seen between different samples. Same probe was used for all the tests in figure 20. Advancements in this method include acoustic emission technique to detect debonding. A microphone is used for picking up acoustic emissions that arise due to crack formation and material failure. Figure 21 shows force displacement curve from a microdebonding test superimposed over the acoustic emissions recorded. A peak can be observed in acoustic emissions indicating debonding.

A variation of this test also exists, commonly known as fibre push-out test. Fibre push-out tests are used more often in recent years [45]. The main difference is that the specimen for push-out test is a thin slice of real composite which is prepared in a

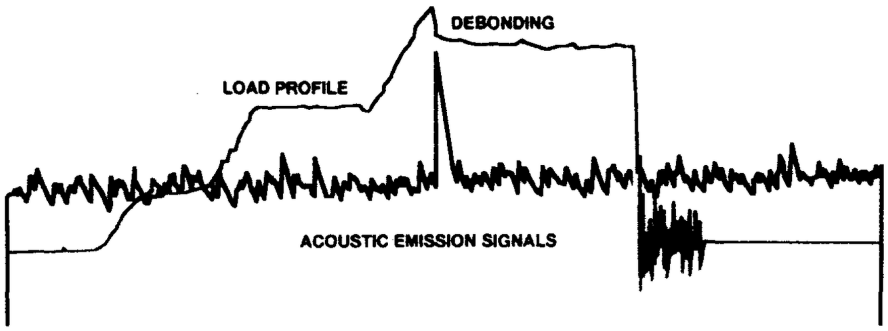

Figure 21: Acoustic emission technique used to detect debonding in microdebonding method [9]

similar way. The micro indenter used is smaller than fibre diameter and during the test, the fibre is debonded along the length and force displacement curve is plotted.In this case, average interfacial shear stress is calculated based on the peak force measured during the test from Equation 17.

$$\tau_s = \frac{P}{2\pi ah} \tag{17}$$

Figure 22 shows schematic and force displacement curve of fibre push-out test from a study conducted in 2010 [10]. One of the main advantages of this method is that the

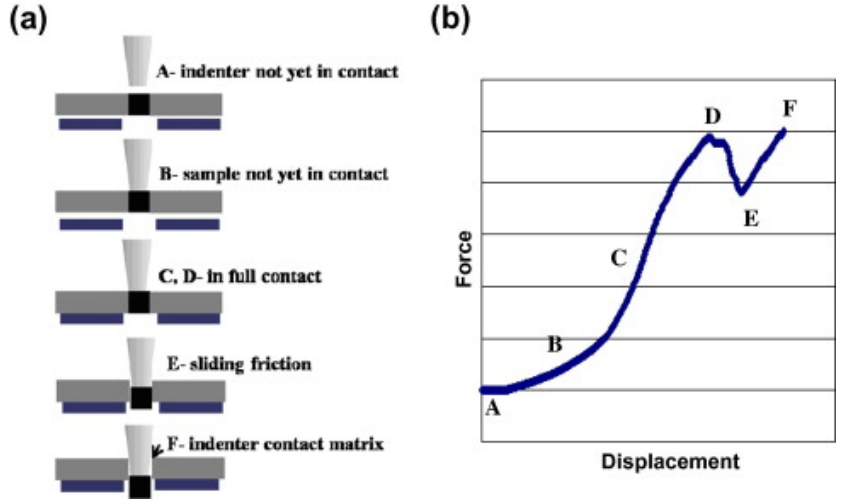

Figure 22: Schematic showing positions of microindenter and corresponding points on force displacement curve [10]

test can be done on actual composite which is manufactured using the conventional process. Moreover, since it can be done on actual composite, it can also be used to study the effect of environment on composite. Several data points can be obtained from single sample, thereby making it time saving. The data collection during the test can be automated, making it even faster. Many issues associated with this test have been rectified over the years. However, Some of the other points that need to be taken into account considering this test are surface defects during specimen preparation due to polishing as these can influence results [8, 29]. Crushing of fibres is a problem considering fibres since they are ideally suited for tensile load and due to low stiffness of polymer matrix, the thin slice is susceptible to bending during the test [27].

2.2.4 Other methods

The methods described so far are the most widely used. However there are some more methods which have been less popular although worth mentioning since for their differences. One of such methods is Broutman test which was first used by Broutman in 1969 [46]. It consists of single fibre composite specimen which is necked towards

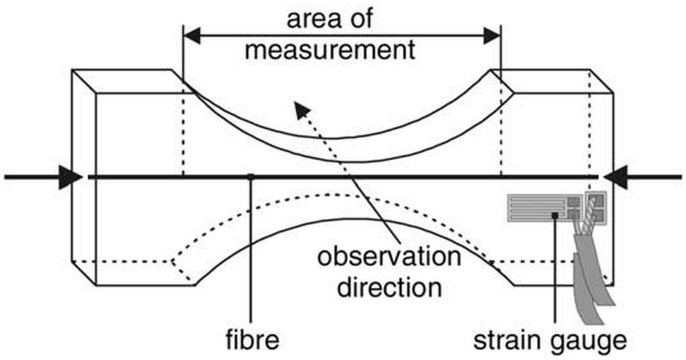

Figure 23: Broutmen test specimen under compression [11]

the centre as shown in Figure 23. The basic principle behind the test is to load a single fibre composite specimen in compression which causes expansion at the centre of the specimen due to Poisson effect. Tensile stress is induced at the interface due to difference in the Poisson's ratio of fibre and the matrix material. The interfacial tensile

stress is calculated using Equation 18.

$$\sigma_{it} = \frac{\sigma_0(\nu_m - \nu_f)E_f}{(1+\nu_m)E_f + (1-\nu_f - 2\nu_f^2)E_m} \tag{18}$$

σ_0 is the axial stress at the minimum cross section of the specimen, ν_m, E_m and ν_f, E_f are Poisson's ratios and elasticity moduli for matrix and fibre respectively [11]. Acoustic emission technique can be used to detect debonding, as shown in Figure 24. Also, photoelasticity can be used if needed [12].

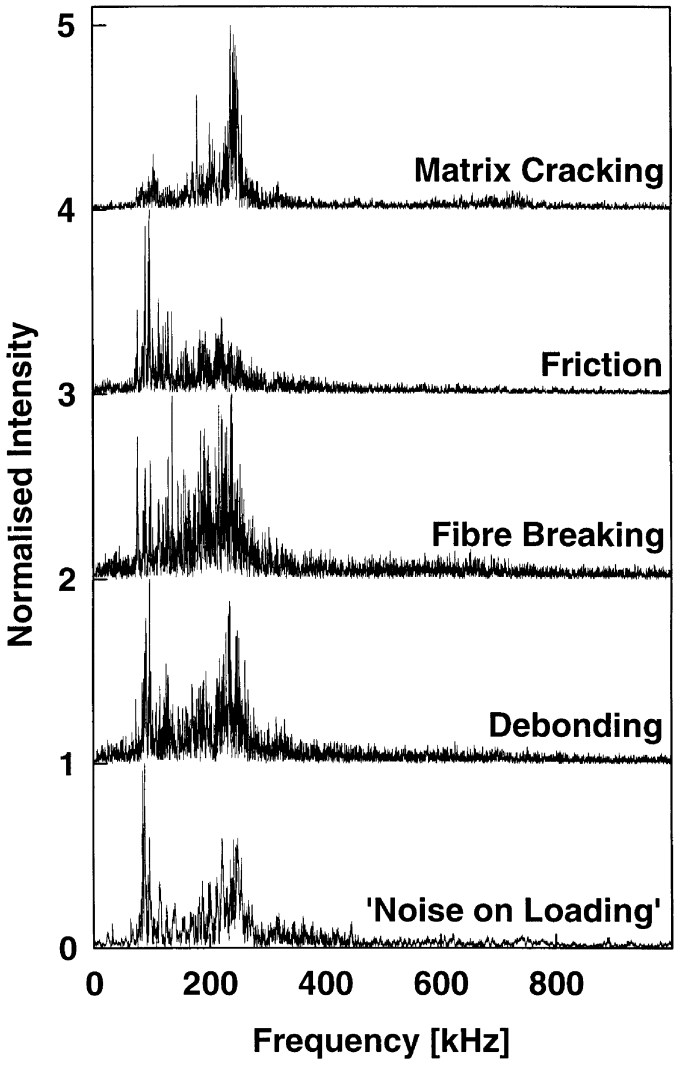

Figure 24: Frequency spectrum signatures associated with events in Broutman test [12]

One of the non conventional tests is single fibre peel test. In this test, small capsules

are filled with matrix material and allowed to gel depending upon the gel time of the resin. Then, a fibre is place carefully over the surface of the resin and put in the oven till the fibres sink by approximately half it's diameter as show in Figure 25. It is important

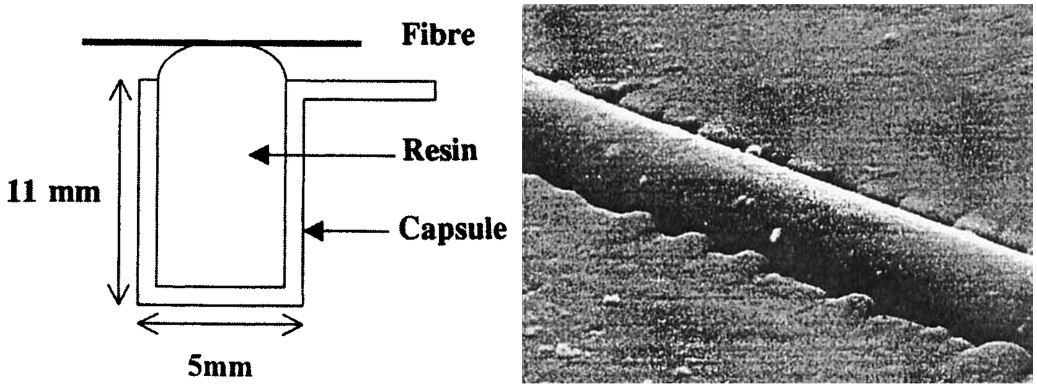

(a) Specimen schematic **(b)** Embedded glass fibre

Figure 25: Single fibre peel test schematic and embedded fibre [13].

that majority of fibre does not sink for the test to be successful. Once the specimen is cured, it is checked with a microscope to ensure more than 60% of fibre is above the surface. The fibre is then peeled using tensile tester. The results obtain from peel tests can be seen in Figure 26. Peel test was conducted at various peel angles and it is

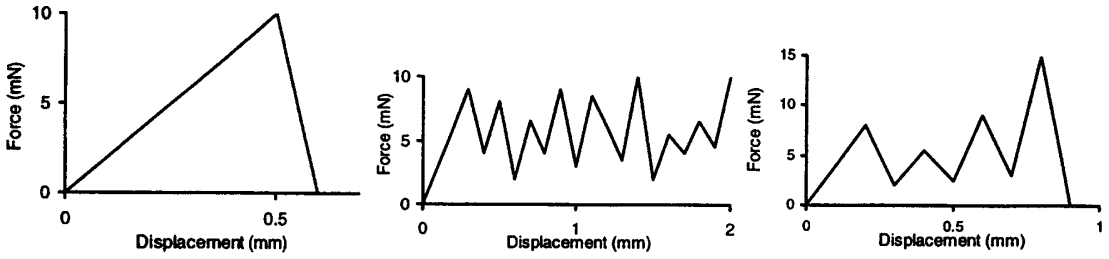

(a) Fibre failure **(b)** Successful peeling **(c)** Partially successful

Figure 26: Typical force displacement plots based on embedded depth of fibre [13]

recommended to carry our peel tests with peel angle of 30 degrees or more. One of

the challenges about this test is that it is difficult to control the embedding depth of fibres in resin [13].

Outwater and Murphy came up with a test in 1969 to measure interfacial strength using a single fibre composite. The specimen consisted of a rectangular shaped matrix specimen with a single fibre embedded longitudinally through the centre as shown in Figure 27. A hole is then drilled through the specimen through the width, going

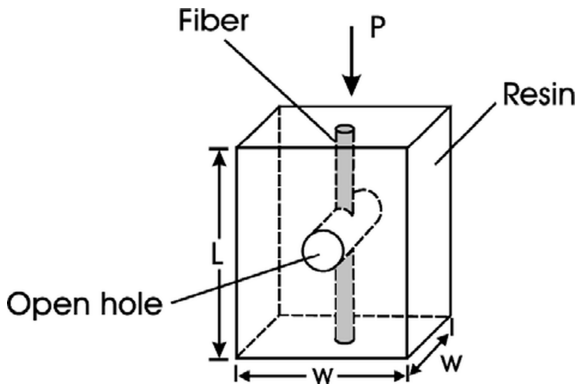

Figure 27: Outwater-Murphy test specimen, schematic and loading [14]

through the fibre. The loading of specimen produces interfacial shear at the fibre ends near the hole due to discontinuity. Test specimen is loaded in compression for the test. The load is increased until debonding is observed visually. The interfacial strength was calculated in terms of debonding fracture energy from Equation 19. The specimen lengths should be kept short in order to avoid buckling [47].

$$G = \frac{\epsilon_r^2 E_f a}{8} \tag{19}$$

ϵ_f is the strain in fibre, E_f is modulus of elasticity of fibre and a is diameter of fibre.

2.2.5 Single fibres methods: Review

All the single fibre methods are reviewed with respect to their applicability, features and constraints in table 2.

Table 2: Micro-mechanical tests comparison

	Microbond/Pull-out test	Fragmentation test	Microdebond/Indentation test
Applicability	More suited for weak interfaces and strong fibres [48].	Suitable for ductile matrices with brittle fibres [5, 49].	Preferred and widely used for ceramic matrix composites [45, 50].
	Suits composites with brittle matrices [5].		
Features	Debond force can be measures and almost any fibre/matrix combination can be used [27, 29].	Specimen loading represents real composite [27].	Allows in situ measurement of debond force in real composite [27].
	Most types of fibres and matrix materials can be used [29, 27].	Single test yields large amount of data [29].	Multiple data points per specimen [29].
	Multiple data points per specimen [27, 29].		

Continued on next page

Table 2 – continued from previous page

	Microbond/Pull-out test	Fragmentation test	Microdebond/Indentation test
Constraints	Embedded length should be less than critical length for successful tests [33].	Strain to failure of matrix should be at least three times of that of fibre [27, 49].	Fibres prone to crushing in compression cannot be used [27] and fibre splitting is a concern [48].
	Not recommended for soft matrix materials since the deformation of matrix material would influence the pull out curve [50].	Transperent matrix material is preferred since it enables to visually observer failure process [29, 51].	Possibility of interfacial defects introduced during specimen preparation for weak interfaces [27, 50].
Other considerations	Meniscus affects measurement of embedded length, contact angle of droplet and blade gap width affects the stress state in the droplet. [27].	Requires fibre tensile strength at gauge length equal to critical length [27].	Poisson effect can lead to higher values of measured interfacial strength [52].
	Does not take into account the effect of surrounding fibres [50]		Specimen is susceptible to bending during test [27].

The main three single fibre methods consisting of pullout, fragmentation and microdebonding are suitable for evaluating the differences in strong and weak interfaces. This has been verified in a round-robin programme involving multiple research laboratories. However, in this programme, all the tests results suffered from data scatter of 25% when the results of different labs were compared and 10% variation for the same lab [28]. Thus, either one of the test can be used for comparative evaluation of interface for different types of fibres of different composites but not for accurate measurement of fibre/matrix adhesion. Certain methods are more suited for some material combinations depending on their individual properties like brittleness, elasticity and expected interfacial strength. All the tests mentioned usually require certain modification to existing material testing equipment available or specially made equipment depending on the method. Fragmentation test requires deriving of material properties from statistical models. The test results for these tests are influenced by test parameters used for testing, these test parameters vary across different laboratories. Until a reliable solution for direct measurement of fibre/matrix interface is developed, it is crucial to verify the results of direct measurements using standardized composite test methods. Also, this helps to check the validity of the direct measurement tests.

Ioncell cellulose fibres are the main interest of this study. Cellulose fibres have greater elonogation to failure compared to glass and carbon fibres. Whereas, fragmentation test requires matrix elongation to failure at least three times of fibre which cannot be met by cellulose fibres. Microdebonding requires reinforcement that can withstand compressive loads without crushing. It would also require special nano-indentation equipment and suffers from problems with specimen preparation like surface defects. Microbond technique on the other hand can be practically used with any type of fibre and matrix combination as long as there isn't considerable matrix deformation observed during the test [5]. Microbond specimens on the other hand are difficult to make with precision owing to it's scale however, it is achievable if the volume of epoxy droplet on the fibre can be controlled precisely. For the above reasons, microbond test was

selected for charactrizing interfacial adhesion for Ioncell cellulose fibres.

2.3 Laminate test methods

These methods use fibres in form of mats, made from bundles of fibres. These methods would classify under multi fibre methods. Off axis mechanical properties like transverse tensile strength and interlaminar shear are heavily influenced by fibre matrix as confirmed in a study by Drzal and Madhukar is 1993 [29]. Hence, tests measuring these properties are good choice for evaluating fibre matrix adhesion. It should be noted that in these tests, often the laminated is subjected to complex stress states along with other effects which have influence on test results as well.

2.3.1 Short-beam shear test

Short beam shear test is also known as interlaminar shear test (ILSS) consists of a short beam specimen as the name suggests. This test is also ASTM (D2344) standard for evaluation of interlaminar shear properties. In this test, a beam with short span is subjected to three point bending in order to achieve failure by shear. The beam dimensions are selected so that interlaminar failure occurs. Length is usually limited to four times the thickness as shown in the Figure 28. Beam theory is used for calculating shear stress in this method, according to which the shear stress, through the thickness of the beam, has parabolic distribution with maximum value at the centre. The maximum shear stress causing failure is calculated using Equation 20. τ_{13} indicates shear through the thickness in vertical plane along the length indicated by suffix, F is applied load and, A is cross-sectional area of beam [6]. If multiple laminates are used for this method, it must be kept in mind the change in stress due to discontinuity [27].

$$\tau_{13} = \frac{0.75F}{A} \tag{20}$$

Usually a unidirectional lamina is used for this test. The failure can occur in tension, compression or shear but only shear failures provide the best results [15]. This test is

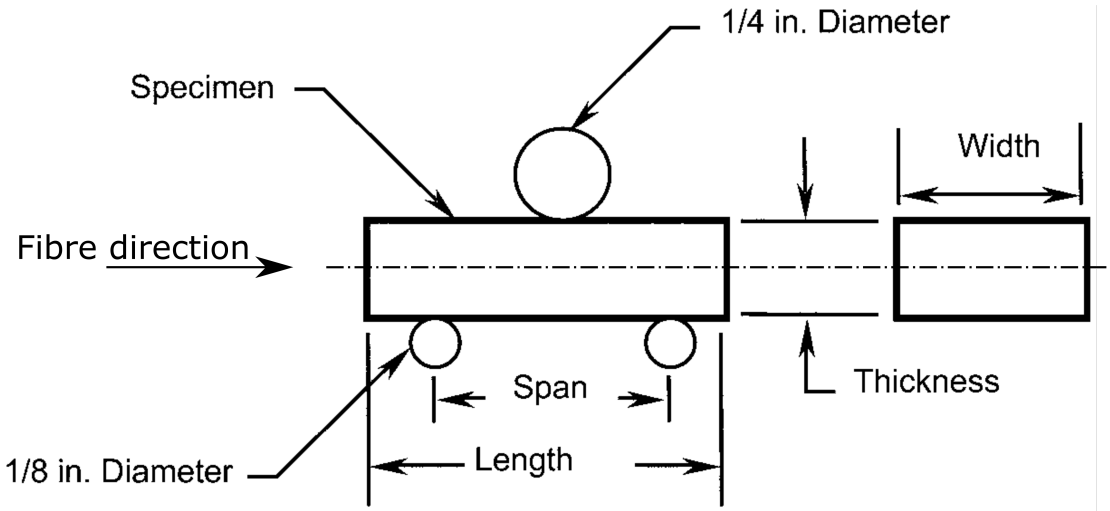

Figure 28: Schematic of short beam shear test [15].

relatively quick, does not require strain gauges for strain measurements and relatively quick, these reasons make this test good for quality evaluation and screening purposes [6].

2.3.2 Iosipescu shear test

Iosipescu test method became ASTM standard in 1993 and is also known as 'V' notched beam method ASTM (5739). This test can be used to test laminate behaviour under shearing loads in any of the three axial directions, depending upon the orientation of fibres in the laminate. For evaluating interlaminar shear properties, the fibre direction is kept parallel to the loading axis for this test. Specimen schematic and loading can be seen in Figures 29a and 29b. The specimen consists of a rectangular lamina with two notches at the centre. The top and bottom edges of the specimen are carefully made parallel to each other so that there are no out of plane bending and twisting loads. A strain gauge is attached to the centre of the specimen between the two notches and used to measure strain during the test. The specimen can be monitored for out of plane stresses by placing a strain gauge on the back face and can be compared with the front. Average shear stress is calculated using the Equation 21 where, A is the cross-sectional area between the notches [6].

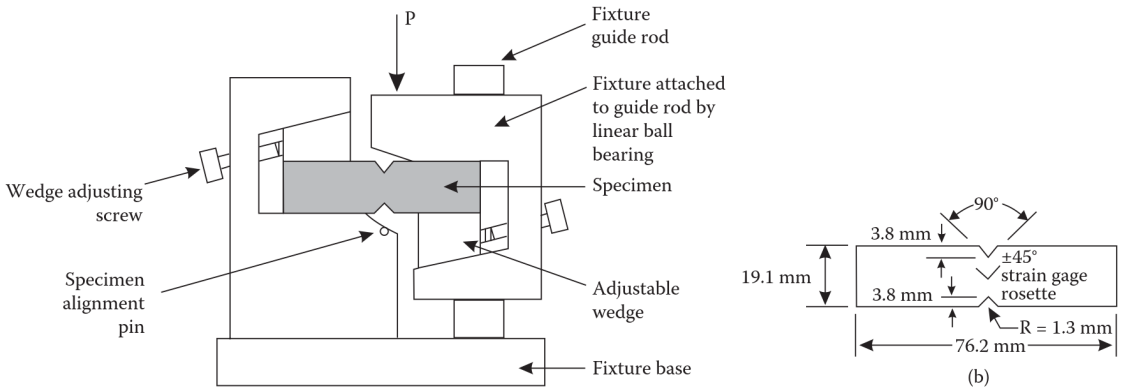

(a) Iosipescu shear test fixture **(b)** Specimen

Figure 29: Schematic of iosipescu fixture and specimen [6]

$$\tau = \frac{F}{A} \tag{21}$$

2.3.3 [±45°] tensile shear test

The ±45° tensile test is a tensile test of a laminate with ±45 layup, each unidirectional fibre mat is arraged at 45° in opposite directions with respect longitudinal axis, so that total angle between them is 90°. 0° indication longitudinal axis. This test is also ASTM (D3518) standard for measuring in-plane shear properties. This test can be used only to determine in-plane shear properties of lamina [15]. The schematic of specimen used is shown in Figure 30. The specimen is subjected to tension using a tensile testing machine however due to the ply configuration, there is a combination of tensile and shear stresses. Each lamina is subjected to tensile stress (σ_{12}) and shear stress (τ_{12}). A bi-axial strain gauge is attached to the specimen as shown in the Figure 30 and the specimen is loaded in tension until it fails while monitoring the load and strain. The shear stress is calculated using Equation 22 which is derived based on classical lamination theory. Simplicity in terms of specimen preparation and can be done with a tensile testing machine are advantages of this test [6].

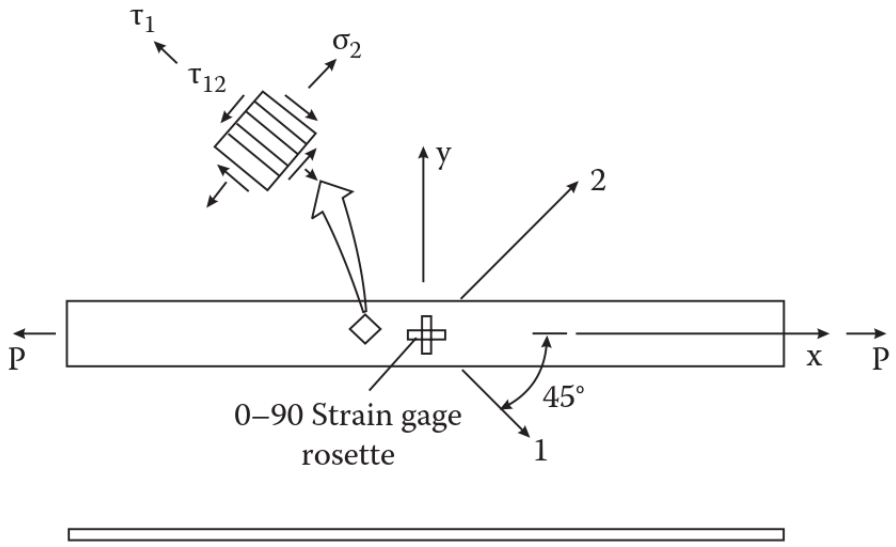

Figure 30: Specimen schematic for ±45° tensile test [6]

$$\tau_{12} = \frac{\sigma_x}{2} \tag{22}$$

2.3.4 Ten-deg Off-axis tensile test

This test was originally proposed by Chamis and Sinclair in 1996 for measuring in-plane shear for composites. A rectangular specimen with a minimum recommended gauge length to gauge width ratio of 14, is used for this test. The recommended dimensions are reduce stress concentration and provide better results. A schematic for test with specimen and fibre configuration is shown in Figure 31. As the name suggests the fibre orientation is ten degrees to the load axis. A strain rosette can be used during testing for measuring strain and can be used for deriving shear modulus. Tensile load on the specimen induces tensile and shear stresses due to coupling effects. The stresses in fibre material co-ordinate system are calculated based on classical lamination theory as shown in the Equations 23, 24 and 25. The failure of the specimen should occur in the ten degree plane only indicating that the interlaminar shear stress has reached it's critical value. Advantages of this test are that it can be done with standard tensile testing procedure and the specimen preparation is simple and inexpensive. The test

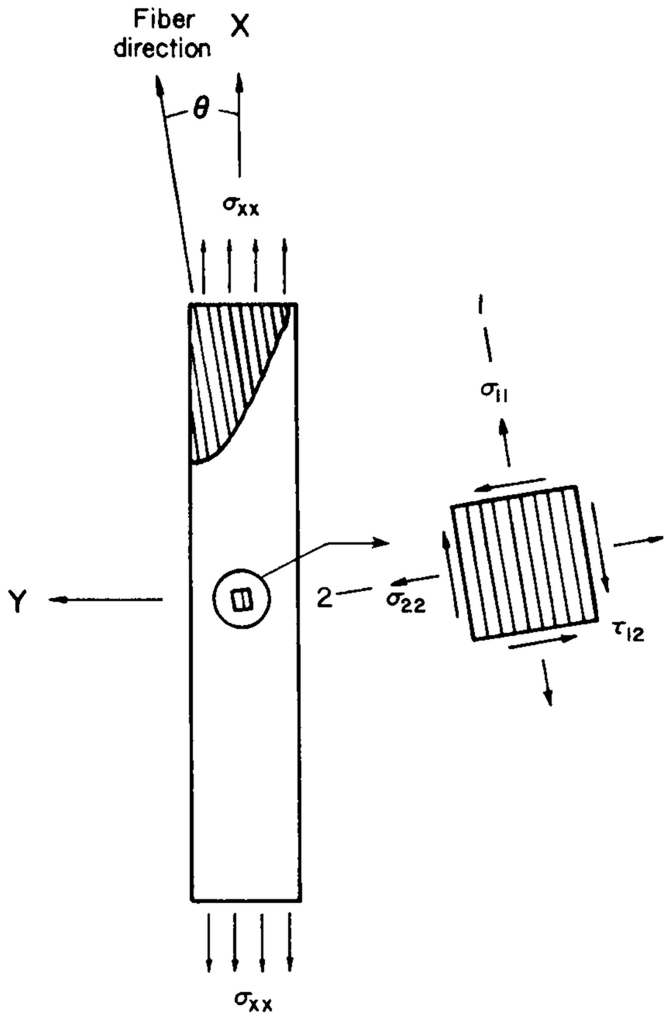

Figure 31: Specimen schematic for ten-deg off axis tensile test [16]

results are sensitive to the fibre orientation and hence it is recommended to have a tolerance of ±10 degrees [53].

$$\begin{aligned} \sigma_{11} &= \sigma_{xx} \cos^2 \theta \\ &= 0.97\sigma_{xx} \end{aligned} \tag{23}$$

$$\begin{aligned} \sigma_{22} &= \sigma_{xx} \sin^2 \theta \\ &= 0.03\sigma_{xx} \end{aligned} \tag{24}$$

$$\begin{aligned} \tau_{12} &= 1/2\sigma_{xx} \sin 2\theta \\ &= 0.171\sigma_{xx} \end{aligned} \tag{25}$$

There are studies on increase of shear strength measured with this test by using oblique tabs. This is the reason for the minimum recommended gauge length to gauge width ratio of 14 recommended by the original authors. The tensile load causes shear as well as tensile strain and the fixed tab ends restrict the shear deformation. This results in non-uniform strain across the width of the specimen and stress concentration near the tabs. The strain induced in a off axis specimen in longitudinal direction is not uniform across the width. Constant strain is obtained along an angle ϕ which is a function of fibre orientation angle θ and can be calculated. Oblique tabs reduce the end stress concentration and restriction to deformation resulting in more uniform strain field reduced error in measurement of shear properties [54].

2.4 Fibre bundle tests

There are only a handful studies that can be found using fibre bundles instead of single fibres or laminates for interfacial adhesion measurements. However it is important to consider these since the cellulose fibres used in the study are only available in fibre bundles and might not be suitable for laminate tests. There are two different methods using fibre bundles, fibre bundle pull-out test and transverse fibre bundle test.

2.4.1 Fibre bundle pull-out test

This method is considered analogous to the single fibre pull-out method [55] and has been used in some studies where single fibre tests were not possible [18] or as an alternative to single fibre tests to check its relevance in interfacial strength evaluation [17]. In this method, a fibre bundle is aligned so that all fibres are straight by applying tension between two ends. Then one or both ends are embedded with matrix material with embedded length depending upon the size of the fibre bundles as shown in Figure 32. The specimen is then cured as per the curing requirements of the matrix material

used. A tensile testing machine is used to test the specimen, load and displacement are monitored until complete debonding of the fibre bundle is complete [17].

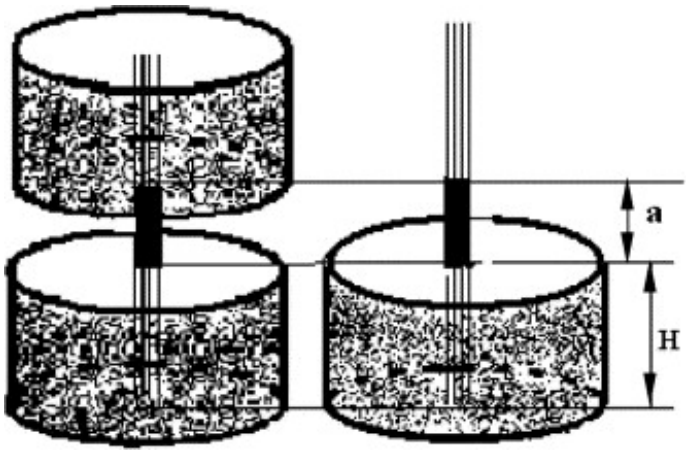

Figure 32: Schematic of single and double end(s) embedded pull-out specimens [17]

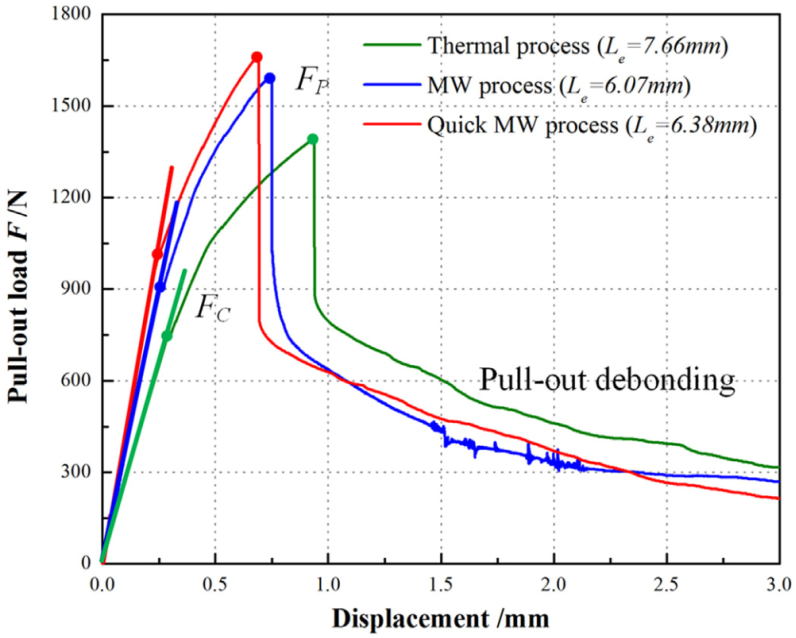

Figure 33: Pull-out curves of carbon fibre and epoxy composites cured with microwave and thermal heating processes [18]

The interfacial strength can be characterized in a similar way as done for the single fibre pull-out test. But instead of fibre diameter, bundle diameter would be used which

is an approximation compared to the pull-out test or the microbond method [55]. The pull-out curves in Figure 33 show differences in interfacial strength depending in the curing method used. The pull-out force for the bundle will be significantly higher than single fibre specimens. Some of the advantages related to this test is that specimen size is relatively large which makes specimen preparation easier. Also regular tensile testing machines can be used due to higher loads and displacement values. The gripping of the specimen can exert additional pressure on fibre bundles resulting on higher interfacial strength. Hence, a way to test without clamping the cylindrical matrix ends might give better results. The interfacial strength calculated using bundle diameter is an approximation and the fibre volume fraction is not taken into account.

3 Microbond method: Setup and testing

3.1 Materials

The aim of this study is Ioncell fibres and it's interfacial strength with commercially used matrix materials. The process used for producing cellulose fibres is named Ioncell and it is developed at Aalto university, school of chemical technology. Commercially available E-glass fibres from OCV reinforcements and Greenlite cellulose fibres from Procher industries are used for comparison. Ioncell cellulose fibres are in form of 30cm long fibre bundles, E-glass fibres and Greenlite cellulose fibres are available in form of unidirectional mat. Bundles can be separated from mats for fibre bundle tests as needed. The fibre properties from tests and data sheets are listed in Table 3.

Property	**Unit**	**E-glass**	**Ioncell**	**Greenlite**
Tensile strength	Mpa	3830 - 3850	-	675
Young's modulus	GPa	78 - 79	-	35
Elongation at break	%	3	8.8	6
Co-efficient of thermal expansion	$\times 10^{-6}$ cm/cm °C	5.9-6.6	-	-

Table 3: Mechanical properties of fibres

For matrix materials, pot life and gel time are crucial for specimen preparation.. Also it may not be possible to prepare all the specimens in one batch and in that case, it is important that the ratio of weights of the components mixed for matrix material are kept identical for different batches. Also processing conditions i.e curing time and temperature should be same for all the batches of test specimens. Araldite LY 5052 is a epoxy resin from Hunstsman and Aropol M105TB is an unsaturated polyester resin from Ashland composites, were selected for matrix materials. Both are commercial resins suitable for hand layup methods, hence they have have long gel times which would

provide enough tie for specimen preparation. Table 4 lists the mechanical properties of matrix materials. These properties can vary depending upon curing times, temperatures and size of composite.

Property	**Unit**	**Araldite 5052**	**Aropol M105TB**
Tensile strength	MPa	82 - 86	55
Young's modulus	GPa	3.5 - 3.6	3.6
Elongation	%	3.1 - 3.7	2

Table 4: Mechanical properties of matrix materials

3.2 Microbond testing

Testing was started with microbond testing first since it requires more time first to develop a method for specimen preparation followed by testing. Also, was dependent on availability of facilities at Tampere university of technology. Out of the matrix materials, epoxy has a longer pot life of 120 minutes, where as polyester resin has gel time of 40 minutes. Also glass fibres being stronger and are 17 microns in diameter compared to Ioncell, which are 11 microns, glass fibres and epoxy matrix were used for initial specimen preparation and tests.

Microbond test results are influenced by droplet size and geometry. Hence, size variation in different specimens should be minimized to reduce data scatter. Different methods for preparing specimens include using a needle [27], thin metallic rod [20] and alumina whisker [56] for transferring small quantities of resin on fibre which would form in to an axis-symmetric droplet. Unfortunately research papers don't go into much detail about the specimen preparation hence developing a process to get consistent specimens was one of the challenges. The problem with the above mentioned methods is that it is difficult to control the amount of epoxy on the tip of needle or whisker, since there is no additional delivery system used for controlling the volume of resin

material on it.

Instead of using the above methods, a hypodermic needle which used for medical purposes, can be used for same purpose. Additionally, it can also help control volume of resin through syringe and are available in multiple sizes with internal diameters as low as 82 microns. The viscosity of resin can limit the minimum diameter that can be used but it can be verified by trial and error. For this study, needles of gauge 25 and internal diameter of 260 micron was used. It was not possible to obtain smaller diameter needles. It is difficult to estimate the required embedded length for microbond test since embedded length since it would depend upon the interfacial adhesion however, data from existing references can be used as a general guide to provide a starting point. Also it is unlikely to find an existing study using the same material combinations and certainly not based on Ioncell fibres. Considering references [27, 33], embedded lengths can range from $100\mu m$ to $200\mu m$ and smaller lengths are possible as well. For first tests with glass fibres and epoxy, aim was to prepare microbond specimens with embedded lengths closer 100 microns. A clean room would be ideally suitable for this since microscopic dust can also influence test results, also separating single fibres from bundles can develop static charge further attracting dust. However fibres being textiles are prohibited at Micronova clean room facilities and it was not possible to use it.

3.2.1 Specimen preparation

The amount of resin required for specimen preparation in this case is extremely small quantity however it is difficult to control mix ratio accurately for very small quantities. Araldite 5052, epoxy resin was mixed with Ardur 5052, hardner. The mix ratio, as per data sheet is 100 parts resin with 38 parts of hardner by weight hence 100 grams of resin was mixed with 38 grams of hardner. The mixture was stirred thoroughly and was allowed to degas. The fibres were separated from bundles and suspended between two points. The fibres were handled only using the ends using gloves so as not to introduce any surface defects. Smallest available sized, one millilitre syringes were used and

smallest were selected since they would offer the most control over epoxy volume coming out. The syringes were first filled with epoxy without the needles and then the needles were attached. Air bubbles, if any present in the epoxy can be removed during this process. A small droplet was allowed to form on the tip by applying force on the plunger and the droplet was made to come in contact with the fibre. Upon withdrawing the needle slowly, a small droplet was formed in the fibre which was then left to cure at room temperature for one day. Once cured, the droplet diameter and embedded length was measured using a microscope.

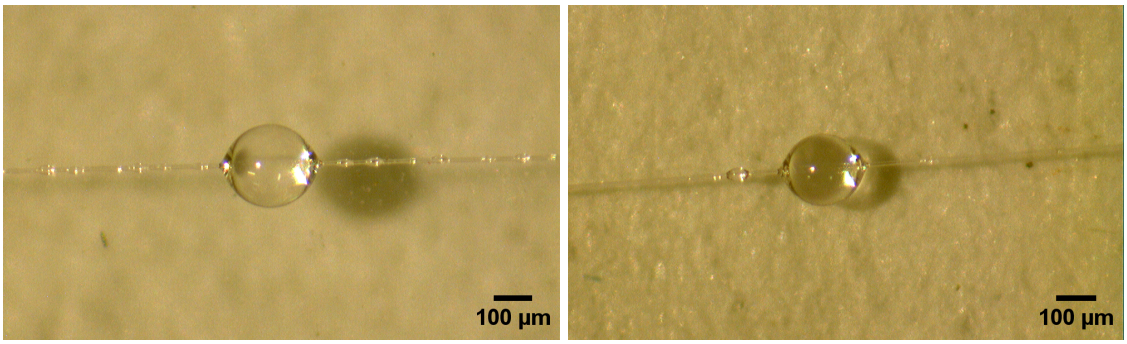

(a) **(b)**

Figure 34: Single fibre specimens made with hypodermic needle

The droplets made using this method were over 150μm. Moreover, since the internal diameter of needle was 260μm, the droplet formed at the needle tip was always greater than or equal to 260μm and resulted in specimens as shown in the Figure 34. Wetting of fibre around the droplet can be seen in Figure 34a which is undesirable and specimen in Figure 34b is better in comparison. There is also risk of damaging fibre due to sharp needle tip and manual operation without any magnification equipment. Other than that, it was only possible to inspect the specimens for unwanted artefacts, after they were cured.

In order to get the smaller sized specimens, a micro-dispensing technique was used to make microbond specimens. This idea originated from a contact angle measurement

study using single fibres by Saketi et. al. [57]. The main advantage of this method was using a micro-dispenser to control the volume of resin at the tip of the needle. The complete assembly consists of micro-dispenser, robotic manipulator controlling the micro-dispenser motion in horizontal and vertical axes and digital microscopes for imaging, observing and recording [58]. The air powered micro-dispenser (Nordon SFD Mikros dispense pen system) is suitable for two part epoxies and adhesives.

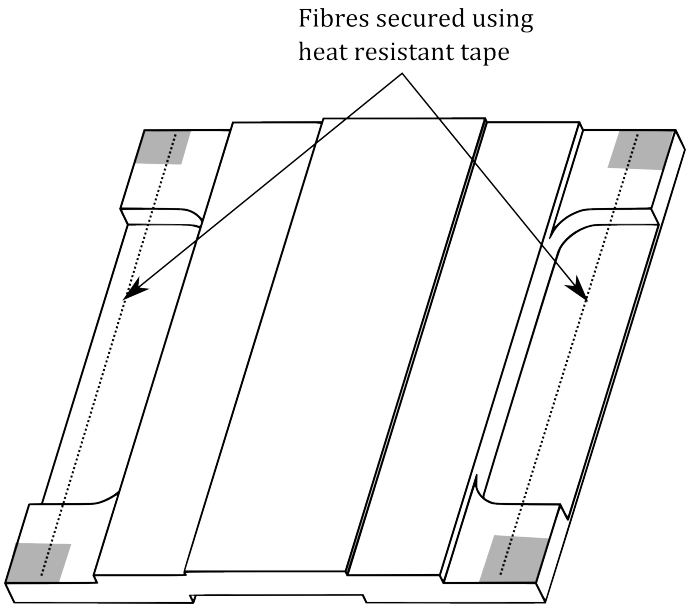

Figure 35: Aluminium mount for micro-dispensing manipulator

The micro-dispenser assembly workspace was limited to 50mm X 50mm area and required machining of an aluminium mount for holding fibres, which could be placed on it and is shown is Figure 35. The size of aluminium mount is 46x46x4mm. The aluminium mounts were first arranged lengthwise and secured with a tape on the middle portion as shown in Figure 36. Then a single fibre separated from the bundle, is placed at one of the sides. The fibre is taped at one end then carefully extended to the other end, until there is no visible sagging. The other end is secured with tape and the procedure is repeated for the other side. The suspended length of fibre on each mount is 30mm. All specimens from a single fibre helps reduce variation in fibre properties and defects over the length. Ideally the specimens should also be as close as possible

to each other to further reduce this.

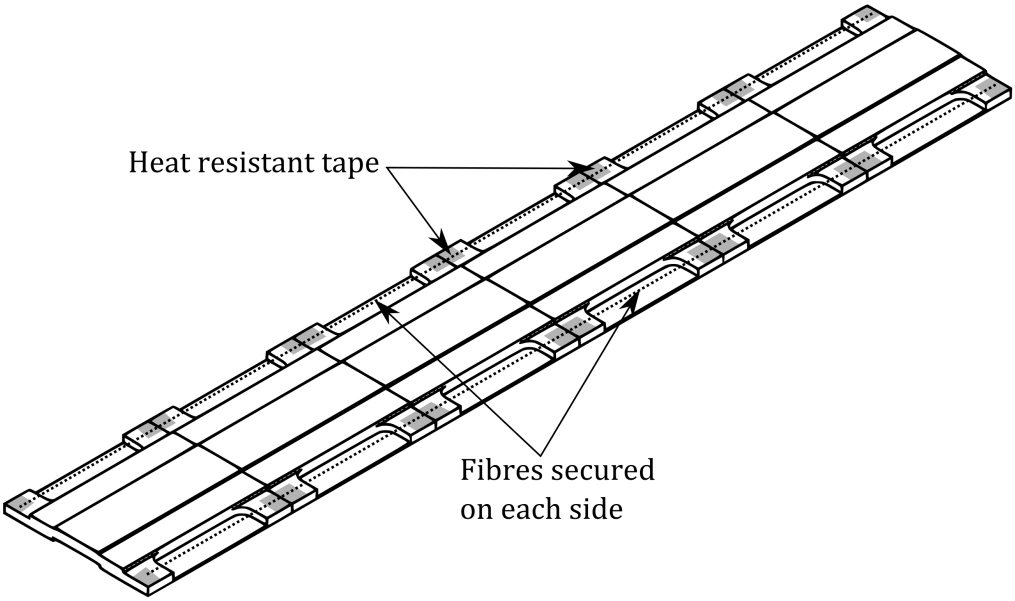

Figure 36: Mounts arranges lengthwise for securing single fibre

Once the fibres are secured and in-place, the individual mounts were separated and stacked as should in the Figure 37. The stacking protects the individual fibres and is easy to carry in a container, since this was done at our lab and then taken to fab2asm lab for micro-dispensing process. The micro-dispensing process was started by setting up the micro-dispenser first. The reservoir of needle (32 gauge and colour code of yellow) was filled with mixed and degassed two part epoxy mixture while ensuring that air bubbles are not formed. Needle was then attached to micro-dispensing pen.

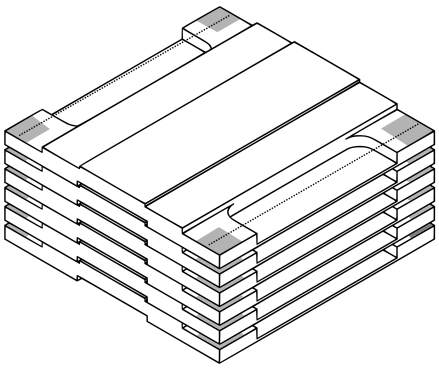

Figure 37: Mounts separated and stacked after securing the fibre

Air pressure is increased till a small hemispherical droplet at the tip. The aluminium mounts with fibre are then placed on work area and using digital microscopes, the droplet at the tip of the needle is passed through the fibre leaving a small amount of epoxy on the fibre as shown in the Figure 38. The droplet formed can be seen from the digital microscope at the time it is formed. It also can be checked for unwanted artefacts around the fibre in case any are present and approximate size can be estimated by comparison to needle tip size which has an outer diameter of 240 microns. Using this method, three microbond specimens were made on single fibre approximately one centimetre apart as needed to suit the testing machine. The testing machine has a travel of 25mm and it is can save time by testing multiple specimens, in this case three, on a single fibre. Two fibre on each mount with six total mounts give total 24 specimens. During the trial some of the specimens were made using needle of different specification since the 32 gauge needle were low on inventory and were all used.

Figure 38: Micro-dispensing process using single glass fibre and epoxy resin

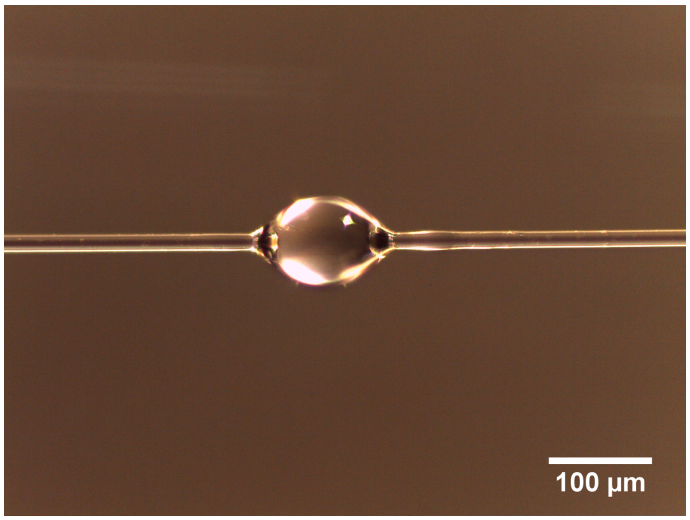

Figure 39: Single fibre glass/epoxy microbond specimen using micro-dispensing technique using 32 gauge needle

The specimens were then left to cure at room temperature for 24 hours and post cured for four hours at 100°C. Following curing, digital images were taken with a calibrated microscope as shown in Figure 39. The embedded lengths were measured from images using ImageJ, which is an open source software for scientific image

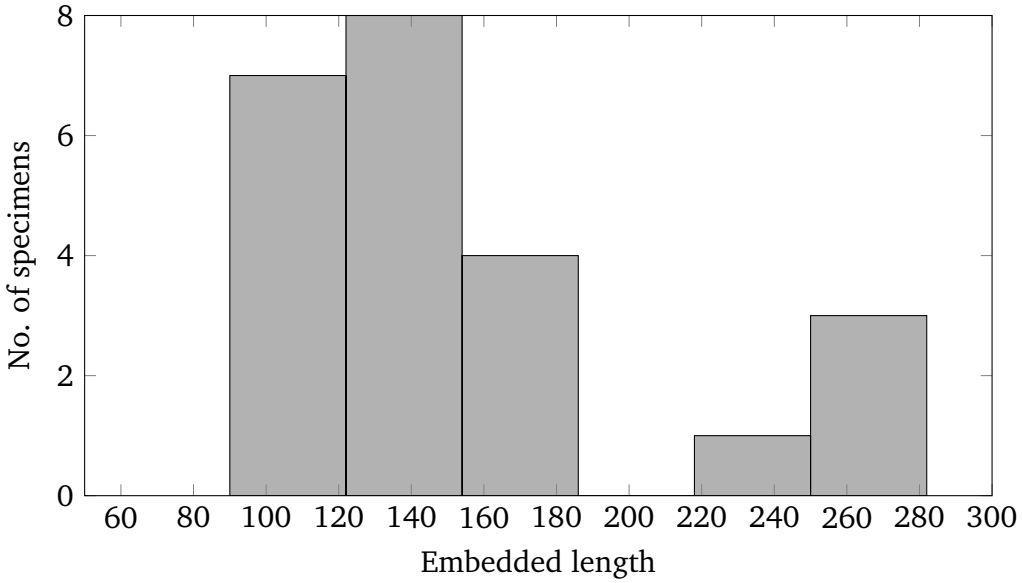

Figure 40: Distribution of embedded lengths across microbond specimens made using micro-dispensing technique

analysis. The minimum embedded length obtained was 95μm and fifteen out of twenty three specimens were less than or equal to 150μm and more would have been possible with the 32 gauge needle. The distribution of embedded length across specimens can be seen in Figure 40. The specimens with embedded lengths greater than 200μm are bigger due to increase in viscosity of epoxy towards the end. Also they start to lose the axis-symmetry due to high viscosity.

The specimens were then taken to Tampere university of technology for testing. The testing apparatus was custom built for microbond tests can be see in in Figure 41. It consists of a load cell, linear actuator, imaging camera interfaced to a computer through an analog input module. Load cell of 3N of 5N can be selected for the test. Test parameters can be adjusted through the graphical use interface on the computer. More details on the testing apparatus can be found in reference [19]. The most challenging part of testing was removing the taped fibres from the mount, securing one end to the gripper and carefully adjusting blade gap. The fibres are removed from the mount by peeling off the tapes, so that fibre is not stressed. Although this could be observed on a screen while performing, it is difficult to make micron scale blade gap adjustments

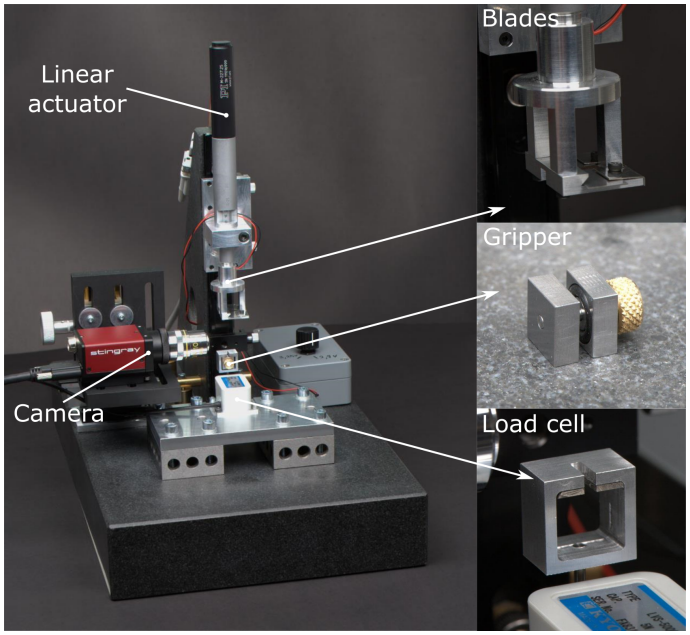

Figure 41: Microbond testing apparatus [19].

manually and can damage the fibre surface. Once the fibre is secured and blade gap adjusted, the test parameters were set and test was started. Force and displacement were recorded during the test and test is allowed to continue until complete debonding is observed. The specimen can be observed on the screen real time as well as can be recorded as video or images.

It was only possible to do a single trial of microbond tests and could not be continued further. Also neither the fibre bundle tests nor laminate tests could be continued due to lack of certain resources and funding.

4 Microbond test results and discussion

A total of four microbond specimens were tested. Displacement rates of 0.05mm/min and 0.1mm/min were used for equal number of specimens. Only four tests could be done because of fibre failure in all four of them. Since there were multiple specimens on the fibre, fibre failure results in shorter lengths which are too short to use with the apparatus. Three specimen failed at the droplet as shown in the Figure 42, while one of the specimen failed at the fibre. Figure 42 shows droplet and the fibre above the blade, the other end of the fibre, which is fixed to the micro-gripper, failed at the droplet.

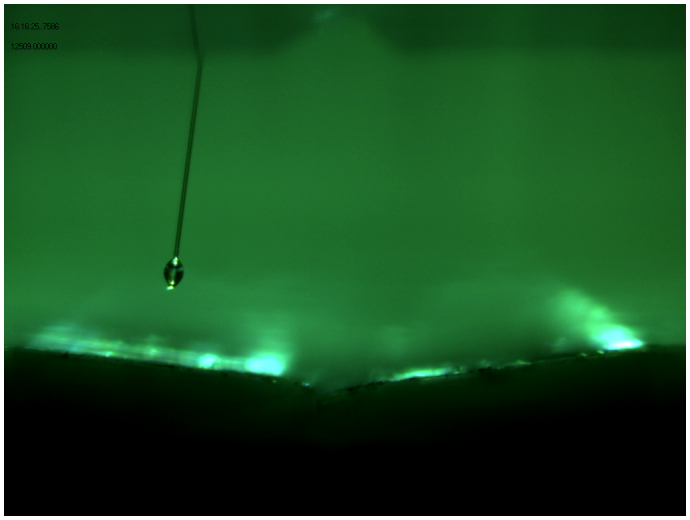

Figure 42: Image of failed specimen taken with camera on microbond testing apparatus

There is a minimum of 44% and maximum of 52% variation in failure load. Tensile strength of glass fibre according to the data sheet is 870mN for 17μm diameter fibre whereas, the failure load is well below that. One of the causes could be due to damage from blade gap adjustment, since the failure location on fibre is near the droplet. Also blade alignment However, it should be noted that the tensile strength is a function of gauge length and so this is an approximation. Also, the sample size to too small to be certain. The test results are summarised in table 5. The force displacement plots obtained are similar to that of existing studies using glass fibre and epoxy upto the

Specimen no.	Displacement rate (mm/min)	Embedded length (μm)	Failure load (mN)
E05	0.1	233	141.9
E08	0.1	112	85.9
E16	0.05	131	132.9
E18	0.05	130	54.2

Table 5: Microbond testing parameters and results

initial debonding. Figure 43 shows force diplacement cure for a successful glass fibre epoxy micobond test. It can be seen that the force displacement plot in Figure 43 upto peak load is similar to the plot from the test shown in Figure 44.

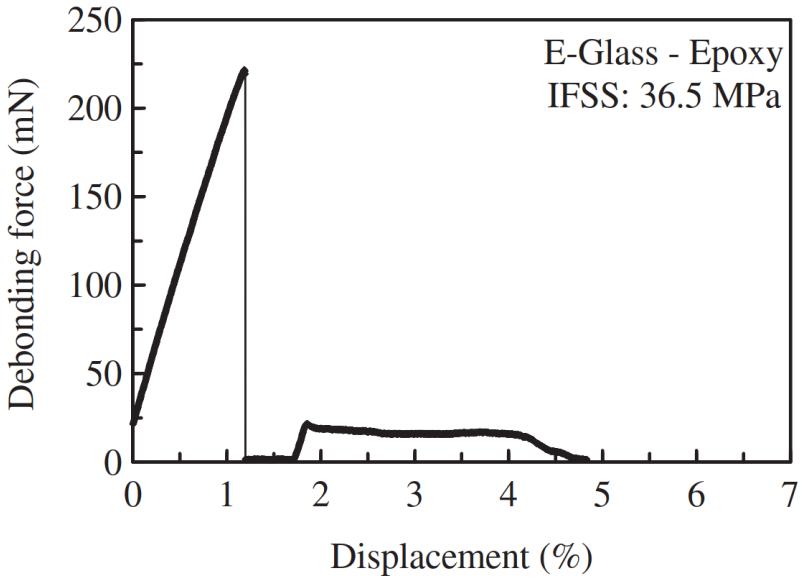

Figure 43: Force displacement plot of a successful glass fibre abd exoxy microbond test [20]

The apparatus does not have provision for direct measurement of blade gap and free fibre length, resulting in variation between specimens. Moreover slight misalignment of blades can be seen on the images from tests. Also slight movement of blades along with specimen was observed, most likely due to flexing of blades. However there was scope

for improvements for all of these issues. The blades could be replaced with a different type offering better alignment. Blade gap and free fibre length could be measured using standard gauges and instruments. Feeler gauge can be used for controlling blade gap and a vernier calliper could be used to measure free fibre length. Micro-dispensing process used can be completely automated once the process variables are established with more trials. This could have resulted in better control over size and geometry of microbond specimens. In case of a successful test, the specimen should be inspected under a microscope to check for failure mode.

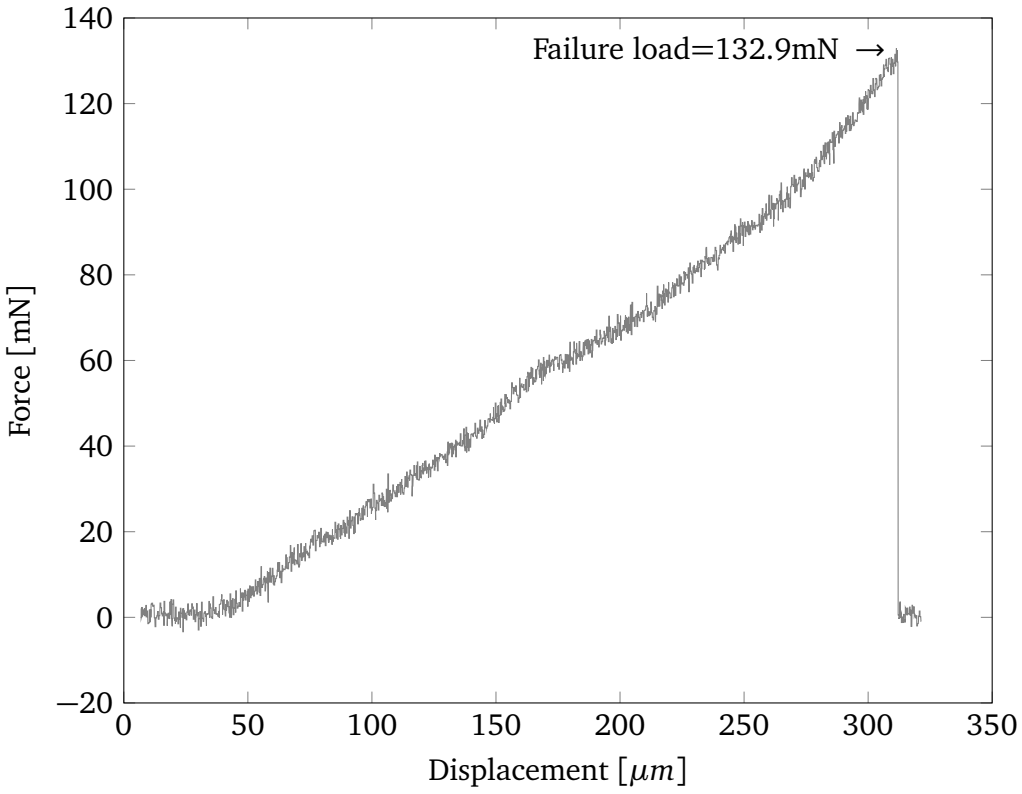

Figure 44: Force vs displacement plot of microbond specimen E16.

5 Conclusion

The aim of this study was reviewing various methods for evaluating fibre/matrix adhesion and employing one of the method to evaluate interfacial strength with Ioncell cellulose fibres. Also, one of the goals was to develop or adopt a technique to evaluate fibre matrix interface in our lab, which doesn't require micro-mechanical tools or special apparatus. A comprehensive review of methods revealed pull out method using microbond technique most suitable for this. This method, although claimed as repeatable and reliable [31] has produced data scatter in results [28], thereby raising doubts on it's accuracy. This introduced further goals, of reserching causes for data scatter and minimising it. An alternate simplified method to approximate interfacial adhesion is fibre bundle pull out test. The concept of fibre bundle pull out is identical to the pull out method but uses fibre bundles and specimen scale is much larger, there by can be tested using commonly uses tensile testing machines. The research however could not be completed and ended at first trial of microbond testing due to lack of resources and funding.

Micrbond technique being a non standard method, required developing a way to prepare specimens and test. After manual procedures similar to the ones found in references, micro-dispensing was ultimately used. Micro-dispensing improved speed of specimen preparation and reduced variation and geometry in microbond specimens, one of the causes for data scatter [27]. The microbond test trial allowed testing of only four glass fibre and epoxy microbond specimens. Neither of the four tests were successful due to premature fibre failure.Improvements for microbond testing are suggested with possible causes of fibre failure. Further work is required on microbond technique with suggested improvements to investigate causes of data scatter. As an alternate method, which can be used with the standard tensile testing machine is the fibre bundle pull out method. This method is less popular hence requires further testing. Fibre bundle pull out tests also could not be done due to budget constraints.

Fiber/matrix adhesion directly influences performance of a composite. Measuring

interfacial adhesion is crucial is useful in researching fibre surface treatments and new fibre materials. There are studies that have investigated the mechanical performance of composites with weak, intermediate and strong adhesion. The performance improves from weak to intermediate where, it reduces and behaves like brittle material as adhesion increases from intermediate to strong [29]. Composites can already be tailored for specific loading, with accurate measurement in adhesion, the material behaviour can be further tailored according to the requirement.

References

[1] Serge Zhandarov and Edith Mäder. An alternative method of determining the local interfacial shear strength from force–displacement curves in the pull-out and microbond tests. *International Journal of Adhesion and Adhesives*, 55(0):37–42, 12 2014.

[2] Derek Hull and TW Clyne. *An introduction to composite materials*. Cambridge university press, 1996.

[3] Michael R. Piggott. *Load bearing fibre composites*. Springer Science and Business Media, 2002.

[4] HL Cox. The elasticity and strength of paper and other fibrous materials. *British journal of applied physics*, 3(3):72, 1952.

[5] Serge Zhandarov and Edith Mäder. Characterization of fiber/matrix interface strength: applicability of different tests, approaches and parameters. *Composites Science and Technology*, 65(1):149–160, 2005.

[6] Leif A Carlsson, Donald F Adams, and R Byron Pipes. *Experimental characterization of advanced composite materials*. CRC press, 2014.

[7] Ben W Kim and John A Nairn. Observations of fiber fracture and interfacial debonding phenomena using the fragmentation test in single fiber composites. *Journal of Composite Materials*, 36(15):1825–1858, 2002.

[8] JF Mandell, JH Chen, and FJ McGarry. A microdebonding test for in situ assessment of fibre/matrix bond strength in composite materials. *International Journal of Adhesion and Adhesives*, 1(1):40–44, 1980.

[9] Eric JH Chen and James C Young. The microdebonding testing system: A method of quantifying adhesion in real composites. *Composites science and technology*, 42(1-3):189–206, 1991.

[10] A Godara, Larissa Gorbatikh, Gerhard Kalinka, A Warrier, O Rochez, L Mezzo, F Luizi, AW Van Vuure, SV Lomov, and I Verpoest. Interfacial shear strength of a glass fiber/epoxy bonding in composites modified with carbon nanotubes. *Composites Science and Technology*, 70(9):1346–1352, 2010.

[11] R Sinclair, RJ Young, and RDS Martin. Determination of the axial and radial fibre stress distributions for the broutman test. *Composites science and technology*, 64(2):181–189, 2004.

[12] C Ageorges, K Friedrich, T Schüller, and B Lauke. Single-fibre broutman test: fibre–matrix interface transverse debonding. *Composites Part A: Applied Science and Manufacturing*, 30(12):1423–1434, 1999.

[13] MA Alimuddin and MR Piggott. Fracture toughness of fiber-polymer interfaces estimated from single fiber peel tests. *Polymer composites*, 20(5):655–663, 1999.

[14] Muhammad U Farooq, Leif A Carlsson, and Betiana A Acha. Determination of fiber/matrix adhesion using the outwater–murphy single fiber specimen. *Engineering Fracture Mechanics*, 76(18):2758–2765, 2009.

[15] Flake C Campbell. *Structural composite materials*. ASM international, 2010.

[16] Marek-Jerzy Pindera, Gaurang Choksi, Jeffrey S Hidde, and Carl T Herakovich. A methodology for accurate shear characterization of unidirectional composites. *Journal of Composite Materials*, 21(12):1164–1184, 1987.

[17] A Zhamu, WH Zhong, and JJ Stone. Experimental study on adhesion property of uhmwpe fiber/nano-epoxy by fiber bundle pull-out tests. *Composites science and technology*, 66(15):2736–2742, 2006.

[18] Jing Zhou, Yingguang Li, Nanya Li, Xiaozhong Hao, and Changqing Liu. Interfacial shear strength of microwave processed carbon fiber/epoxy composites

characterized by an improved fiber-bundle pull-out test. *Composites Science and Technology*, 133:173–183, 2016.

[19] Voitto Känkänen. Yksittäiskuidun adheesiontestauslaite. Bachelor's thesis, Tampere university of technology, 2015.

[20] Ramesh-Babu Adusumalli, Moritz Reifferscheid, Hedda K Weber, Thomas Roeder, Herbert Sixta, and Wolfgang Gindl. Shear strength of the lyocell fiber/polymer matrix interface evaluated with the microbond technique. *Journal of Composite Materials*, 46(3):359–367, 2012.

[21] David W Green, Jerrold E Winandy, and David E Kretschmann. Wood handbook: Wood as an engineering material. *General technical report FPL-GTR-113, US Department of Agriculture, Forest Service, Forest Products Laboratory, Madison, WI*, 1999.

[22] Sunil K. Ramamoorthy, Mikael Skrifvars, and Anders Persson. A review of natural fibers used in biocomposites: Plant, animal and regenerated cellulose fibers. *Polymer Reviews*, 55(1):107–162, 2015.

[23] Jiying Fan, Elias Nassiopoulos, James Brighton, Alain De Larminat, and James Njuguna. New structural biocomposites for car applications. In *Society of Plastics Engineers-EUROTEC 2011 Conference Proceedings, Barcelona, Spain*, pages 14–15, 2011.

[24] Dilpreet S Bajwa and Sujal Bhattacharjee. Current progress, trends and challenges in the application of biofiber composites by automotive industry. *Journal of Natural Fibers*, 13(6):660–669, 2016.

[25] AK Mohanty, M. Misra, and G. Hinrichsen. Biofibres, biodegradable polymers and biocomposites: an overview. *Macromolecular Materials and Engineering*, (276-277):1–24, 2000.

[26] Mark Hughes. Defects in natural fibres: their origin, characteristics and implications for natural fibre-reinforced composites. *Journal of Materials Science*, 47(2):599–609, 2012.

[27] PJ Herrera-Franco and LT Drzal. Comparison of methods for the measurement of fibre/matrix adhesion in composites. *Composites*, 23(1):2–27, 1992.

[28] MJ Pitkethly, JP Favre, U Gaur, J Jakubowski, SF Mudrich, DL Caldwell, LT Drzal, M Nardin, HD Wagner, L Di Landro, et al. A round-robin programme on interfacial test methods. *Composites Science and Technology*, 48(1):205–214, 1993.

[29] LT Drzal and M Madhukar. Fibre-matrix adhesion and its relationship to composite mechanical properties. *Journal of Materials Science*, 28(3):569–610, 1993.

[30] Nikolaos E Zafeiropoulos. *Interface engineering of natural fibre composites for maximum performance*. Elsevier, 2011.

[31] Bernard Miller, Pierre Muri, and Ludwig Rebenfeld. A microbond method for determination of the shear strength of a fiber/resin interface. *Composites Science and Technology*, 28(1):17–32, 1987.

[32] Béla Pukánszky. Interfaces and interphases in multicomponent materials: past, present, future. *European Polymer Journal*, 41(4):645–662, 2005.

[33] Ramesh-Babu Adusumalli, Hedda K Weber, Thomas Roeder, Herbert Sixta, and Wolfgang Gindl. Evaluation of experimental parameters in the microbond test with regard to lyocell fibers. *Journal of reinforced plastics and composites*, 2010.

[34] BJ Carroll. Equilibrium conformations of liquid drops on thin cylinders under forces of capillarity. a theory for the roll-up process. *Langmuir*, 2(2):248–250, 1986.

[35] CT Chou, U Gaur, and B Miller. The effect of microvise gap width on microbond pull-out test results. *Composites science and technology*, 51(1):111–116, 1994.

[36] GD Andreevska and Yu A Gorbatkina. Adhesion of polymeric binders to glass fiber. *Industrial & Engineering Chemistry Product Research and Development*, 11(1):24–26, 1972.

[37] P Järvelä, KW Laitinen, J Purola, and P Törmälä. The three-fibre method for measuring glass fibre to resin bond strength. *International journal of adhesion and adhesives*, 3(3):141–147, 1983.

[38] S. Zhandarov. Is there any contradiction between the stress and energy failure criteria in micromechanical tests? part i. crack initiation: Stress-controlled or energy-controlled? *Composite interfaces*, 5(5):387–404, 1998.

[39] S. Zhandarov. Is there any contradiction between the stress and energy failure criteria in micromechanical tests? part iii. experimental observation of crack propagation in the microbond test. *Journal of Adhesion Science and Technology*, 19(8):679–704, 2005.

[40] Serge F Zhandarov, Edith Mäder, and Oleg R Yurkevich. Indirect estimation of fiber/polymer bond strength and interfacial friction from maximum load values recorded in the microbond and pull-out tests. part i: local bond strength. *Journal of adhesion science and technology*, 16(9):1171–1200, 2002.

[41] A Kelly and amd WR Tyson. Tensile properties of fibre-reinforced metals: copper/tungsten and copper/molybdenum. *Journal of the Mechanics and Physics of Solids*, 13(6):329in1339–338in2350, 1965.

[42] Stefanie Feih, Karen Wonsyld, Daniel Minzari, Peter Westermann, and Hans Lilholt. Establishing a testing procedure for the single fiber fragmentation test. Technical report, Forskningscenter Risø, 2004.

[43] P Feillard, G Désarmot, and JP Favre. A critical assessment of the fragmentation test for glass/epoxy systems. *Composites science and technology*, 49(2):109–119, 1993.

[44] Tadashi Ohsawa, Akira Nakayama, Minoru Miwa, and Akira Hasegawa. Temperature dependence of critical fiber length for glass fiber-reinforced thermosetting resins. *Journal of Applied Polymer Science*, 22(11):3203–3212, 1978.

[45] N Chandra and H Ghonem. Interfacial mechanics of push-out tests: theory and experiments. *Composites Part A: Applied Science and Manufacturing*, 32(3):575–584, 2001.

[46] LJ Broutman. Measurement of the fiber-polymer matrix interfacial strength. In *Interfaces in composites*. ASTM International, 1969.

[47] John O Outwater and Michael C Murphy. The influences of environment and glass finishes on the fracture energy of glass-epoxy joints. *The Journal of Adhesion*, 2(4):242–253, 1970.

[48] M Narkis, EJH Chen, and RB Pipes. Review of methods for characterization of interfacial fiber-matrix interactions. *Polymer Composites*, 9(4):245–251, 1988.

[49] Nina Graupner, Joraine Rößler, Gerhard Ziegmann, and Jörg Müssig. Fibre/matrix adhesion of cellulose fibres in pla, pp and mapp: a critical review of pull-out test, microbond test and single fibre fragmentation test results. *Composites Part A: Applied Science and Manufacturing*, 63:133–148, 2014.

[50] Maya Jacob, Seena Joseph, Laly A Pothan, and Sabu Thomas. A study of advances in characterization of interfaces and fiber surfaces in lignocellulosic fiber-reinforced composites. *Composite Interfaces*, 12(1-2):95–124, 2005.

[51] Tim Huber and Jörg Müssig. Fibre matrix adhesion of natural fibres cotton, flax and hemp in polymeric matrices analyzed with the single fibre fragmentation test. *Composite Interfaces*, 15(2-3):335–349, 2008.

[52] MR Piggott. Why interface testing by single-fibre methods can be misleading. *Composites Science and Technology*, 57(8):965–974, 1997.

[53] Christos C Chamis and James H Sinclair. Ten-deg off-axis test for shear properties in fiber composites. *Experimental Mechanics*, 17(9):339–346, 1977.

[54] M Kawai, M Morishita, H Satoh, S Tomura, and K Kemmochi. Effects of end-tab shape on strain field of unidirectional carbon/epoxy composite specimens subjected to off-axis tension. *Composites Part A: Applied Science and Manufacturing*, 28(3):267–275, 1997.

[55] V Cech, P Janecek, T Lasota, and J Bursa. A fiber-bundle pull-out test for surface-modified glass fibers in gf/polyester composite. *Composite Interfaces*, 18(4):309–322, 2011.

[56] JP Craven, R Cripps, and C Viney. Evaluating the silk/epoxy interface by means of the microbond test. *Composites Part A: Applied Science and Manufacturing*, 31(7):653–660, 2000.

[57] Pooya Saketi, Juha Hirvonen, Yuli Lai, Christian Ganser, Christian Teichert, Joakim Jarnstrom, Pedro Fardim, and Pasi Kallio. Automated drop-on-fiber contact angle measurement using a microrobotic platform. *Nordic Pulp & Paper Research Journal*, 29(2):225–231, 2014.

[58] Ali Shah, Bo Chang, Sami Suihkonen, Quan Zhou, and Harri Lipsanen. Surface-tension-driven self-alignment of microchips on black-silicon-based hybrid template in ambient air. *Journal of Microelectromechanical Systems*, 22(3):739–746, 2013.